Snoring Sounds Analysis for the Assessment of the Upper Airway Anatomy and Fluid Accumulation in the Neck during Sleep

By

Shumit Saha

A thesis submitted to the Faculty of Graduate Studies of

The University of Manitoba

In partial fulfillment of the requirements of the degree of

Master of Science

Department of Biomedical Engineering

University of Manitoba

Winnipeg

Snoring Sounds Analysis for the Assessment of the Upper Airway Anatomy and Fluid Accumulation in the Neck during Sleep

Shumit Saha

Master of Science

Department of Biomedical Engineering
University of Manitoba

2016

Abstract

Fluid accumulation in the neck due to rostral fluid shift during sleep can increase the tissue content surrounding the upper airway and worsen the severity of obstructive sleep apnea (OSA), a respiratory disorder occurs due to the upper airway narrowing. Since snoring sounds are generated by the vibrations of upper airway due to its narrowing, purpose of this thesis was to explore the potential of the snoring sounds features to monitor upper airway anatomy (area or length) during sleep and tissue content. A modified subject-specific acoustic model for snoring generation was proposed and compared with measured results from recorded snoring of human participants. We found the only factor that significantly contributed to snoring intensity was upper airway narrowing, while snoring spectral frequencies were negatively correlated with increased tissue content and OSA severity. These results encourage the potential use of snoring sounds analysis to assess upper airway narrowing and tissue content.

Acknowledgments

I am very grateful to my supervisors, Dr. Zahra Moussavi and Dr. Azadeh Yadollahi, for their help, support, and guidance during my M.Sc. program. It has been an honour to work and learn from these esteemed scientists. Thanks to their efforts, I have grown tremendously in both my professional and personal life.

I am very thankful to Dr. Adrian West, Dr. Jitendra Paliwal and Dr. Sherif Sherif for serving on my thesis committee and for their useful comments and suggestions. I am also greatly thankful to Dr. Douglas Bradley for his valuable comments in my thesis.

I am also grateful to my colleagues Bojan Gavrilovic, Derek Zhi, Peyman Hadi, Mahsa Taheri, Mehrnaz Shokrollahi, and Daniel Vena for their help in all aspects of my research. I would also like to thank the other members of both the Sleep team at Toronto Rehab and BME team at University of Manitoba for their continued support and feedback throughout my research.

I would like to acknowledge the Manitoba Graduate Scholarship (MGS) for providing me the funding throughout my M.Sc. study period.

I am also greatly indebted to my uncle and aunt, Subal Saha and Ratna Karmaker, for their invaluable support throughout my M.Sc. program.

I would like to acknowledge the unconditional love and support of all my family members, especially of my sister, Shusmita Saha.

Lastly, I would like to dedicate this thesis to my mother, Shumana Saha, whose patience and constant prayers help to overcome all the hardship of my life.

I thank God the Almighty for his mercy and forgiveness throughout my life.

Table of Contents

List of Tables

List of Figures

List of Abbreviations

AASM- American Academy of Sleep Medicine

AHI- Apnea Hypopnea Index

BIA- Bioelectrical Impedance Analysis

MRI- Magnetic Resonance Imaging

NC- Neck Circumference

NFV- Neck Fluid Volume

N1- Non Rapid Eye Movement Sleep Stage 1

N2- Non Rapid Eye Movement Sleep Stage 2

N3- Non Rapid Eye Movement Sleep Stage 3

OSA- Obstructive Sleep Apnea

PSG- Polysomnography

REM- Rapid Eye Movement

UA-XSA- Upper Airway Cross Sectional Area

UA-Length- Upper airway length from vellum to glottis

Chapter 1

1 Introduction

1.1 Motivation

Obstructive sleep apnea (OSA) is a common breathing disorder during sleep affecting around 4-14 % of men and 2-7% of women above the age of thirty [1]. Previous studies have shown that OSA causes hypersomnolence, cognitive impairment [2], increases the risk of stroke by 4 times [3], heart failure by 3 times [4, 5], and car and work related accidents by 2-10 times [6-8]. In the United States alone, economic costs of sleep apnea are estimated to be more than $65 billion annually [9]; and it is increasing, as the population ages and becomes more obese and more sedentary. Furthermore, because of the costly sleep studies in sleep laboratory, people do not want to undergo in a sleep study. As a result, more than 90% of patients who are at risk of OSA remain undiagnosed [10].

OSA occurs due to repetitive collapses of upper airway resulting in pauses in breathing for more than 10 seconds (apnea) or occurrence of abnormally low breathing flow (hypopnea) during sleep [1]. However, the cause of airway collapse during sleep is still unclear and understanding the mechanism for collapse can result in alternative and personalized treatments [11]. Several factors such as increased tissue content in the neck including increased pharyngeal fat and edema [1], or reduction in pharyngeal dilator muscle tone at sleep onset[1] may contribute to the upper airway narrowing during sleep. Furthermore, rostral fluid shift from the legs into the neck during sleep can increase the neck fluid volume (NFV) and further increase the upper airway resistance and collapsibility [12, 13] . The gold standard techniques to monitor the upper airway anatomy during sleep (i.e. its narrowing, length, airway wall thickness) are based on MRI or endoscopy

which are costly, inconvenient, and could change the normal patterns of breathing. Therefore, developing a convenient and non-invasive technique to monitor the upper airway anatomy during sleep could improve the management of OSA.

Respiratory or snoring sounds analysis is a non-invasive and convenient way to investigate variations in the upper airway anatomy and monitor its obstruction during sleep. Furthermore, acoustic features of the respiratory or snoring sounds may change with the tissue composition surrounding the upper airway due to the rostral fluid shift. Therefore, the primary goals of this thesis are to investigate the association between snoring sounds features and variations in the upper airway anatomy and changes in NFV during sleep. These results could be used to develop algorithms based on snoring sounds for monitoring the upper airway narrowing during sleep.

1.2 Background

1.2.1 Variations in Upper Airway Anatomy and Snoring Sounds Analysis

Previous studies have shown that narrowing in the upper airway is the main reason of the generation of snoring sounds [14, 15]. Narrowing in upper airway can increase airflow speed during inspiration. According to the Bernoulli's theorem, this increased airflow speed causes a pressure drop across the upper airway [14]. This pressure drop leads to more negative intraluminal pressure in the upper airway, which further narrows the upper airway and leads to increased speed of airflow in the upper airway. This sequence of events causes the turbulence of airflow and leads to the vibration of the tissues in the upper airway (i.e. soft palate, pharyngeal wall) and induces the snoring sounds [14].

Since snoring is highly associated with OSA, previous studies have done a great amount of effort to develop algorithms based on snoring sounds for diagnosis of OSA [16-20]. Maimon et al.

analyzed snoring sounds from 1643 simple snorers and found that increases in the snoring sound intensity were highly associated with severity of OSA [18]. Padilla et al. analyzed snoring sounds from 19 patients and found that first snoring segment after an apnea event had more power in high frequencies than other snoring segments. They further found that the power ratio of above to below 800 Hz could be a potential tool to differentiate simple snorers from snorers with OSA [19]. Fiz et al. studied 10 OSA patients and 7 simple snorers and found patients with OSA had significantly lower peak frequency than simple snorers [17]. Ng et al. investigated snoring sounds of 30 patient with severe sleep apnea and 10 snorers without sleep apnea and found snoring from OSA patients exhibited higher first formant than those from simple snorers [21]. Azarbarzin et al. analyzed the bispectral features of snoring sounds and classified OSA patients from simple snorers with 93% accuracy by using higher order features and energy of snoring sounds [22]. Ng et al. performed the nonlinear analysis of snoring sounds to predict OSA severity and found that peak frequency and peak sum frequency of wavelet bi-coherence analysis could be two potential diagnostic markers of OSA [23]. Although these studies have demonstrated that snoring sounds can be used for screening OSA, however the effects of physiological and anatomical changes of upper airway during sleep on snoring sounds features has not been investigated in details.

Several studies have implemented the finite element models [24], mechanical models[25, 26] or electrical equivalent of the upper airway[27] to simulate the generation of breathing sounds and to assess the effects of upper airway narrowing and collapsibility on the acoustic features of breathing sounds. But, very little emphasis was given on modelling an upper airway for snoring sounds generation to assess the effects of upper airway anatomy on snoring sounds features [28,

29]. Therefore, a detailed study to understand the effects of underlying mechanism of upper airway anatomy during sleep on acoustic features of snoring sounds is necessary.

1.2.2 OSA and Fluid Accumulation in the Neck

Although there's around 10% of the general population has sleep apnea [1]; its prevalence is increased almost five fold in fluid retaining conditions like heart failure or renal disease [30-36]. Previous studies have provided significant evidence that rostral fluid shift from the legs to the neck while sleeping increases the fluid accumulation in the neck and play a vital role in upper airway narrowing [37-39]. They have shown that increases in the fluid volumes of the jugular veins could cause an inward displacement of the lateral walls of the upper airway, increase pressure from outside of the upper airway and consequently narrow the upper airway. Furthermore, increase hydrostatic capillary pressure in surrounding tissues of the upper airway could filtrate transcapillary fluid into the interstitial tissues of the neck and increase interstitial edema and eventually result in increases of upper airway collapsibility [40]. Thus, they showed that fluid accumulation in the neck increases the NFV, edema of the pharyngeal tissues and consequently narrows the upper airway which worsens the OSA severity [41-45]; whereas reducing fluid retention in the legs in the daytime and preventing its rostral shift in the night can minimize OSA [38, 39].

Furthermore, previous studies have shown that in older men (> 40 yr old), the intravenous infusion of about 2 liters of normal saline during sleep significantly increased the OSA severity; assessed by the apnea-hypopnea index (AHI), the occurrence of apneas and hypopneas per hour of sleep [46]. Conversely, in patients with end stage renal disease, removing around 2 liters of fluid by ultrafiltration can reduce the AHI by 36% [47]. These studies are further supported by

the postoperative worsening of OSA severity [48, 49], where patients receive significant amounts of fluid intravenously during and following surgery [48].

These studies have proven the concept that fluid accumulation in the neck could result in the increases of pharyngeal tissue edema, cause significant variations in the upper airway anatomy and play a vital role for development of OSA.

1.2.3 Fluid Accumulation in the Neck and Snoring Sounds analysis

There are several ways of measuring the NFV during sleep such as MRI and bioelectrical impedance analysis. However, these methods are inconvenient and difficult to perform during sleep. Conversely, snoring sounds analysis is a convenient method to predict the upper airway anatomy. Since snoring sounds are generated due to the vibrations of the upper airway tissues and will be transmitted to the microphone placed at the neck through the pharyngeal tissue, the natural vibrations of the tissues surrounding the upper airway can affect the frequency spectrum of the snoring sounds. Therefore, variations in snoring sounds features can be used to assess the changes in tissue edema and NFV during sleep.

1.3 Objectives

The objectives of this study can be listed as follows:

i. To develop a subject-specific acoustic model of the upper airway for snoring sounds generation and propagation to investigate the effects of variations in the upper airway anatomy during sleep on snoring sounds features.
ii. To investigate the effects of changes in the NFV on temporal and spectral features of the snoring sounds.

1.4 Organization of the Thesis

The thesis is organized as follows:

This thesis has two major sections focused on 1) the subject-specific acoustic model of the upper airway for snoring sounds generation and 2) investigation of changes in NFV on snoring sounds features.

In Chapter 2, a subject-specific acoustic model of the upper airway is demonstrated. This study has five major parts: a) acoustic modelling of the upper airway for snoring sounds generation; b) investigating the relationship between upper airway anatomy and modeled snoring sounds data; c) extraction and measurement of the acoustic features of snoring sounds that obtained from the recording of breathing sounds during sleep study; d) investigating the association of measured snoring sounds features with changes in the upper airway anatomy during sleep; e) comparison between the modelling results and the measured results of recorded snoring sounds. All of them are briefly described in Chapter 2. The work presented in Chapter 2 has been published in:

Shumit Saha, T. Douglas Bradley, Mahsa Taheri, Zahra Moussavi & Azadeh Yadollahi, A Subject-Specific Acoustic Model of the Upper Airway for Snoring Sounds Generation. Scientific Reports 6, Article number: 25730 (2016), doi:10.1038/srep25730 [50].

In Chapter 3, the association between the variations in the NFV during sleep and snoring sounds features is demonstrated. This study has two parts: a) investigating the relationship between NFV and snoring sounds features; b) development of a simple spring and mass model that mimics the effects of fluid accumulation in the neck on snoring sounds features. The work presented in Chapter 3 is in process of submitting to a journal.

Finally, Chapter 4 outlines the conclusion and future objectives of this research.

In Appendix A, the details of the temporal and spectral features of the snoring sounds are demonstrated that described in chapter 2.

Appendix B represents the details of the modified subject-specific acoustic model that is described in chapter 2. In the appendix, the equations and the values of the different parameters of the model are presented.

Appendix C represents the basics of the bio-electrical impedance measurement and fluid volume estimation. The derivation of the fluid volume estimation equation is represented in the appendix.

Appendix D represents the detailed study protocol and data measurement of the study.

Chapter 2

2 A Subject-Specific Acoustic Model of the Upper Airway for Snoring Sounds Generation to Assess the Upper airway Anatomy by Snoring Sounds Features

The content of this chapter was published as a peer reviewed journal article: Shumit Saha, T. Douglas Bradley, Mahsa Taheri, Zahra Moussavi & Azadeh Yadollahi, *A Subject-Specific Acoustic Model of the Upper Airway for Snoring Sounds Generation*, Scientific Reports 6, Article number: 25730 (2016), doi:10.1038/srep25730 [50].

Except for the formatting and some organizational and stylistic improvements, the content of this chapter is almost identical to the aforementioned publication. Contribution of authors is as follows: Shumit Saha proposed the modified model of the upper airway for snoring sounds generation, manually annotated the snoring segments from breath sounds and performed the signal processing and statistical analysis. Azadeh Yadollahi and Zahra Moussavi supervised all the aspects of this work and edited and reviewed the paper. T Douglas Bradley and Azadeh Yadollahi designed the experimental protocol and acquired all the physiological data. Mahsa Taheri helped in the manual annotation of snoring segments.

This chapter demonstrates a modified upper airway model for snoring sounds generation to understand the effects of upper airway area and length on the acoustic features such as intensity or resonant frequencies of snoring sounds.

2.1 Introduction

Snoring is present in 20% to 40% of the general population[51], and is associated with obesity, nasal obstruction, use of alcohol and cigarettes[52]. Snoring sounds are generated by vibration of pharyngeal tissues due to the narrowing and the consequent increases in the turbulent airflow in the upper airway[14]. Several factors such as increased pharyngeal fat[1], reduction in pharyngeal dilator muscle tone at sleep onset[1], and rostral fluid shift from the legs to the neck [53] may contribute to the upper airway narrowing during sleep. However, the underlying mechanisms of the upper airway narrowing are multifactorial and may change from night to night in the same individual [11]. Consequently, it is difficult to use imaging techniques such as MRI or endoscopy to investigate variations in the upper airway during sleep such as it's narrowing, collapsibility, or airway wall thickness[54].

On the other hand, snoring sounds can be recorded conveniently with a microphone placed on the neck, or in the vicinity of the patient in the room. Snoring can be a sign of obstructive sleep apnea (OSA)[55]; a common respiratory disorder present in approximately 10% of adult population. OSA is characterized by repetitive complete or partial collapse of the upper airway during sleep[1]. Consequently, most of studies on acoustic analysis of snoring sounds focused on the association between OSA severity and a variety of snoring sounds features such as intensity[18], power spectral measures[17], bi-spectral and non-linear measures [23], formant frequencies [21] and temporal features. However, very little emphasis was placed on the effects of variations in the upper airway anatomy during sleep on snoring sounds features. Liu et al. used

a 3D model of the human head to identify the source of snoring sounds; however, the model was computationally intensive and highly dependent on having an accurate 3D model of the head for every individual [28]. Ng et al. developed an electrical equivalent model of the upper airway to investigate the effects of upper airway narrowing on spectral features of snoring sounds[29]. They observed general agreement between the spectral features of simulated and actual recorded snoring sounds in 40 subjects. However, since they did not measure the upper airway cross-sectional area (UA-XSA) in their population, a detailed subject-specific validation of the model to assess the effects of upper airway narrowing on the characteristics of recorded snoring sounds was missing.

To address this gap, we aimed to develop a subject-specific acoustic model of the upper airway for snoring sounds generation. Based on the physics of sounds generation in a tube, we hypothesized that snoring sounds intensity will be directly related to narrowing of the upper airway, and the resonant frequency of snoring sounds will be inversely related to the length of upper airway. To have a subject-specific model, we measured the neck circumference (NC), upper airway length (UA-Length) and UA-XSA of human participants and incorporated them in the model for snoring sounds generation. For every individual, the modelling results for snoring sounds intensity and resonant frequencies were compared with those measured from recorded snoring sounds in the same individual during sleep

2.2 Results

2.2.1 Baseline Characteristics of participants

Twenty men participated in a daytime sleep study and their sleep was assessed with a full in-laboratory polysomnography (PSG) (See methods section for details). Table 2.1 shows the

baseline characteristics of the subjects. Although this was a daytime study, participants slept for an average of 150 minutes (Table 2.2), and 14 out of 20 had at least one full sleep cycle, including both rapid eye movement (REM) and non-REM sleep stages. Participants spent most of the sleep time in stage 2 of non-REM (N2) sleep (Table 2.2). The participants had a wide range of OSA severity, as assessed by apnea-hypopnea index (AHI, number of apneas and hypopneas per hour of sleep). Nine subjects had no or mild sleep apnea (AHI < 15), five had moderate sleep apnea ($15 \leq AHI < 30$) and six had severe sleep apnea ($AHI \geq 30$).

Table 2.1 : Characteristics of the participants (n=20)

Variable	**Mean ± SD**
Age, years	45.1 ± 11.4
Height, cm	176.9 ± 6.3
Weight, kg	79.0 ± 10.7
Body Mass Index, kg/m^2	25.4 ± 3.05
Neck circumference , cm	41.8 ± 2.9
Upper Airway Cross-Sectional Area, cm^2	2.6 ± 0.6
Velum to Glottis length, cm	9.1 ± 1.8
Systolic Blood Pressure, mmHg	110.6 ± 8.5
Diastolic Blood Pressure, mmHg	76.0 ± 8.3

Table 2.2: Sleep structure (n=20)

Variable	Mean ± SD
Total sleep time, min	150.1 ± 46.1
N1 sleep, %	18.0 ± 10.4
N2 sleep, %	57.2 ± 15.1
N3 sleep, %	11.5 ± 12.9
REM sleep, %	10.7 ± 8.1
Sleep efficiency, %	74.7 ± 15.0
Total AHI, /h	27.6 ±25.8
Obstructive AHI, /h	25.5 ± 25.7
Central AHI, /h	2.0 ± 2.67

Before and after sleep, while subjects were supine, NC was measured with a measuring tape, and UA-Length and average of UA-XSA (both from velum to glottis) were measured with acoustic pharyngometry (See methods section for details). From before to after sleep, there were significant increases in NC (ΔNC: 0.5 ± 0.3 cm, $p<0.001$) and decreases in UA-XSA (ΔUA-XSA: -0.4 ± 0.3 cm^2, $p<0.001$). As we have shown before, these changes could be due to rostral fluid shift from the legs to the neck while supine [56]. Airway wall thickness which was estimated based on NC and UA-XSA, increased from before to after sleep (Δ: 0.2±0.08 cm, $p<0.001$). There was a strong correlation between reductions in UA-XSA and increases in airway wall thickness ($r=-0.73$, $p<0.001$).

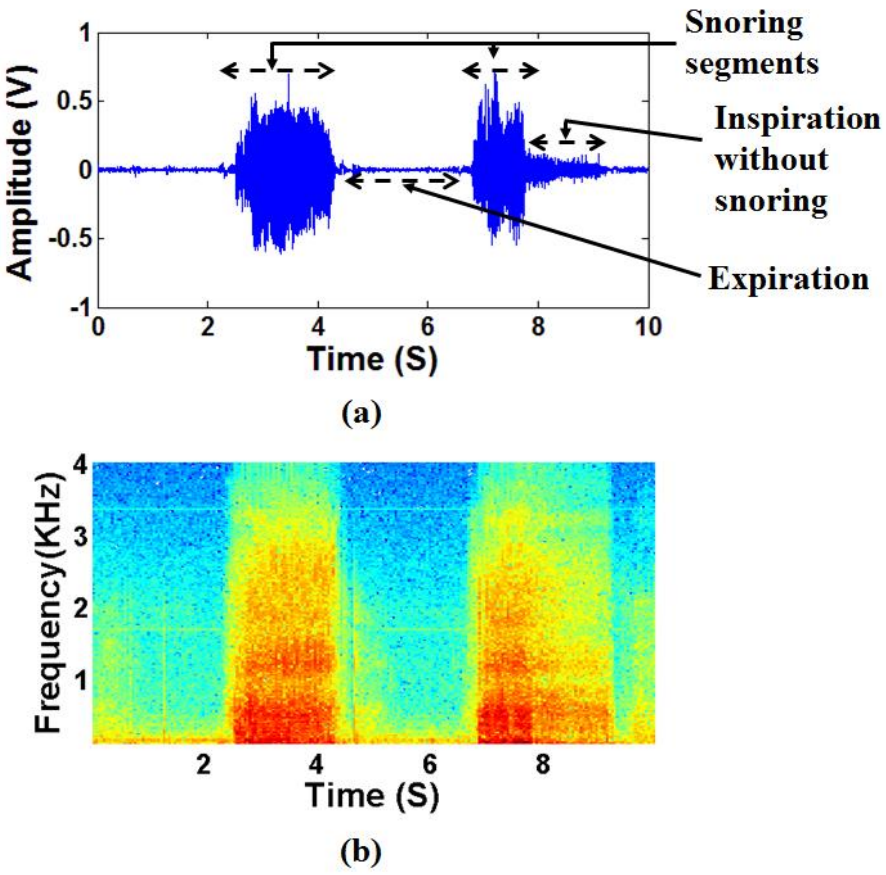

Figure 2.1: Segmentation of snoring sounds from breath sounds: (a) Extracted snoring segments from a 10 seconds recording of breath sounds; (b) Spectrogram of the extracted snoring segments as presented in (a). In all frequency bands, snoring sounds intensity were larger than those of the inspiratory and expiratory breath sounds without snoring.

2.2.2 Snoring Sounds Features

Snoring and breath sounds were recorded with a microphone attached to the neck (See methods section for details). Snoring segments were extracted manually by listening to the sounds and observing them in the time and frequency domains. Fig. 2.1 shows a 10-second sample of recorded breath sounds, along with the manual annotation of the snoring segments. While both inspiratory and expiratory snoring were detected, since the snoring mechanisms may be different during inspiration and expiration and inspiratory snoring are more common, only inspiratory snoring were investigated in this study.

For every individual, 342±223 inspiratory snoring segments were extracted (134.2±96.0 snoring per hour of sleep). The snoring segments were band-pass filtered in the frequency range of 100-4000 Hz to remove the effects of heart sounds in the low frequency range as well as extraneous noises in the high frequency range [57, 58]. Various features in the temporal and spectral domains were extracted from the snoring sounds (See methods section for details). The total snoring time in each sleep stage normalized by the time spent in each sleep stage (snoring time index) was similar for different sleep stages ($p>0.10$), as well as for non-REM vs. REM sleep ($p>0.10$). The measured average power of snoring sounds was 38.2±5 dB in the frequency band of 100-4000 Hz. There was a positive correlation between the measured relative power of snoring sounds in the frequency range of 150-450 Hz and the AHI (Fig. 2.2, $r=0.48$, $p=0.039$).

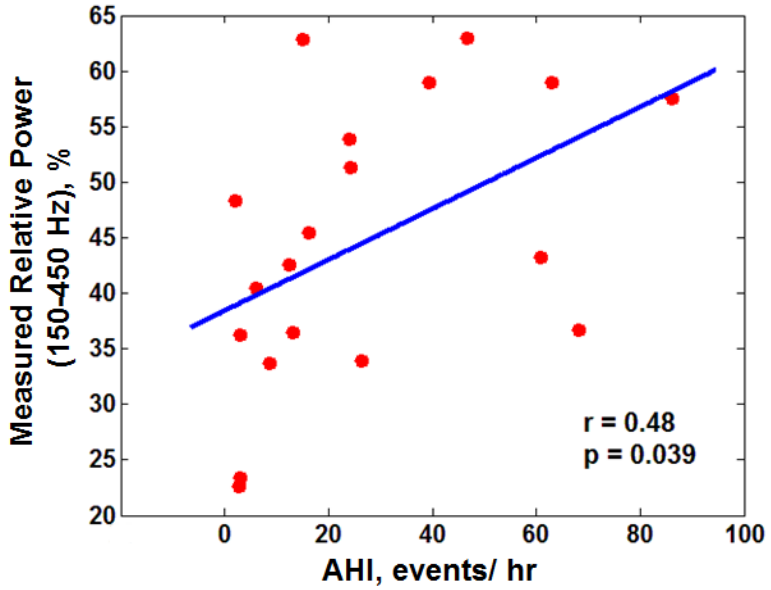

Figure 2.2: Relationship between AHI and measured relative power of snoring sounds (assessed by Pearson Correlation Coefficient): Increases in AHI were significantly correlated with the increases in the measured relative power of snoring sounds within 150–450 Hz frequency range.

2.2.3 Acoustic model of the upper airway for snoring sounds generation and propagation

Based on the theory of sounds generation in a collapsible tube[15], and the basics of changes in the oral cavity for vowel articulations[59], we assumed a simplified two-compartmental model for snoring sounds generation and propagation (Fig. 2.3). These compartments included, first, the snoring sounds generation within the upper airway, due to vibration of the soft palate and uvula, and/or of the tissues between the soft palate and epiglottis; and second, the entire upper airway, which was modeled as a collapsible tube through which the pressure fluctuations due to snoring are propagated to the microphone located on the suprasternal notch.

We modeled the snoring source vibration as a sinusoid signal with its frequency equal to the measured pitch frequencies of the recorded snoring sounds (See methods section for details). For every individual, the pitch frequency of each snoring segment was estimated and averaged for entire sleep. The mean and standard deviation of the measured pitch frequencies among all subjects was 102.1±20.6 Hz. For the upper airway response, we developed an electrical equivalent model of a collapsible tube [27, 60, 61] (See methods section for details). The parameters of the upper airway model, such as resistance and capacitance, were defined based on UA-Length, UA-XSA and airway wall thickness. To validate the model, resonant frequencies and average power of snoring sounds based on modelling and measured data were estimated and compared.

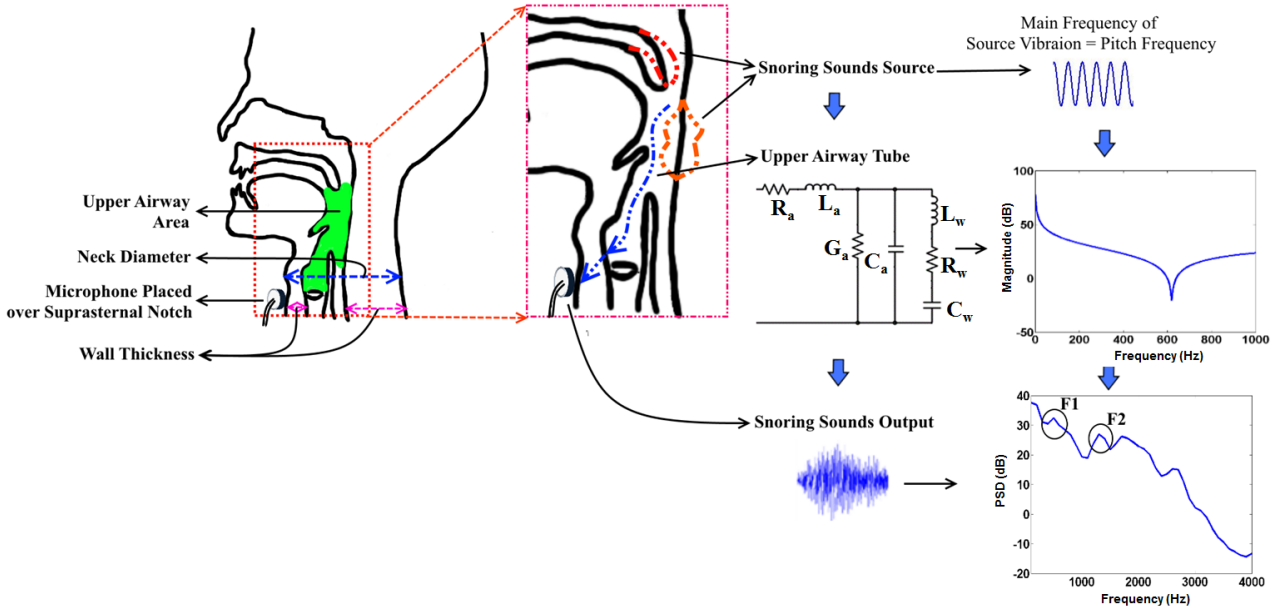

Figure 2.3: An overview of the proposed block scheme of snoring sounds generation and propagation along with the acoustic model of upper airway: Snoring sounds is generated by the vibration of soft palate or pharyngeal wall, then would propagate through the upper airway and then recorded by the microphone placed over the suprasternal notch. The main frequency of snoring sounds source is analogous to the calculated pitch frequency of snoring sounds. The upper airway was modeled by the electrical equivalent circuit of a collapsible tube with non-rigid wall (Ra, resistance; La, inertance; Ca, compliance; Ga, conductance; Lw, wall inertance; Rw, wall resistance; Cw, wall compliance) using measured upper airway area, neck diameter, wall thickness showed in the anatomy of upper airway. The power spectral density (PSD) of the snoring segment extracted from the recorded data with the marking of formant frequencies is also shown.

2.2.4 Effects of upper airway anatomy on the resonant frequencies of snoring sounds

For every subject, resonant frequencies of snoring sounds were calculated as the averages of first and second formants (F1 and F2, respectively) of all recorded snoring sounds. The average and standard deviation of measured F1 and F2 among all subjects were 572.1±122.6 Hz and 1626.1±168.7 Hz, respectively. On the other hand, for each subject, we used the baseline measurements of UA-XSA, wall thickness, and UA-Length before sleep to estimate F1 (modeled F1). There was a strong correlation between the modeled and measured F1 (Fig. 2.4-a, r=0.58, p=0.01). Also, based on the Bland-Altman analysis (Fig. 2.4-b), there was a strong agreement between modeled and measured F1.

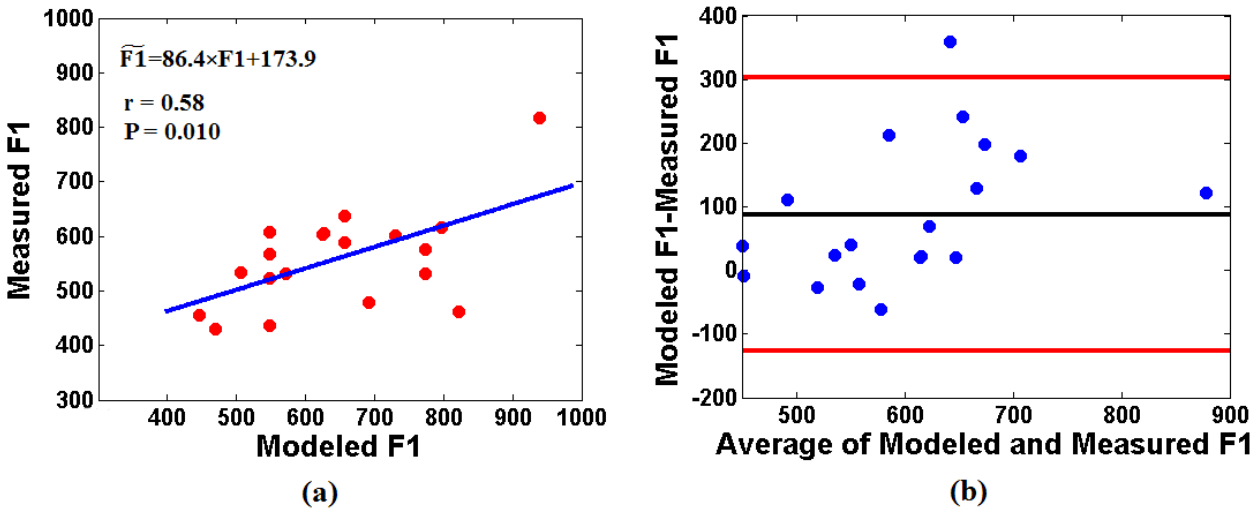

Figure 2.4: Agreement between modeled and measured F1 of the snoring sounds: (a) Scatterplot of the F1 of the recorded snoring sounds (measured F1) and F1 simulated from the upper airway tube model (modeled F1) along with the linear regression equation of modeled and measured F1, where is the measured F1; (b) Bland–Altman plot: the black line indicates the average difference and the red lines present the mean±1.96 of standard deviation (boundaries of 95% confidence interval) of the difference between modeled and measured F1.

2.2.4.1 Results obtained from the modeled snoring frequencies

We calculated the effects of changes in UA-XSA, UA-Length and wall thickness on resonant frequencies of the model. The modelling results showed that length of the upper airway was inversely related to the modeled F1. Increasing the UA-Length from 7.0 cm to 12.5 cm, modeled F1 decreased from 800 Hz to 450 Hz ($r=-0.98$, $p<0.001$). On the other hand, there were no significant correlations between modeled F1 and variations in the UA-XSA or airway wall thickness ($p>0.05$ for both).

2.2.4.2 Results obtained from measured snoring frequencies

There was a significant and negative correlation between the measured F1 of all snoring segments during sleep and the UA-Length before sleep ($r=-0.55$, $p=0.015$). Previous studies have shown that UA-Length is longer in patients with OSA than in those without OSA [62, 63]. Based on recorded snoring sounds, there were significant and negative correlations between AHI and measured F2 (Fig. 2.5-a, $r=-0.49$, $p=0.030$), AHI and measured spectral centroid of snoring sounds in the frequency range of 1200-1800 Hz (associated with F2[64]) (Fig. 2.5-b, $r=-0.59$, $p=0.006$), and AHI and measured spectral centroid in 450-600 Hz (associated with F1[64]) (Fig. 2.5-c, $r=-0.50$, $p=0.023$).

Therefore, both modelling and measured results suggested that there was an inverse relationship between resonant frequencies of the snoring sounds and UA-Length.

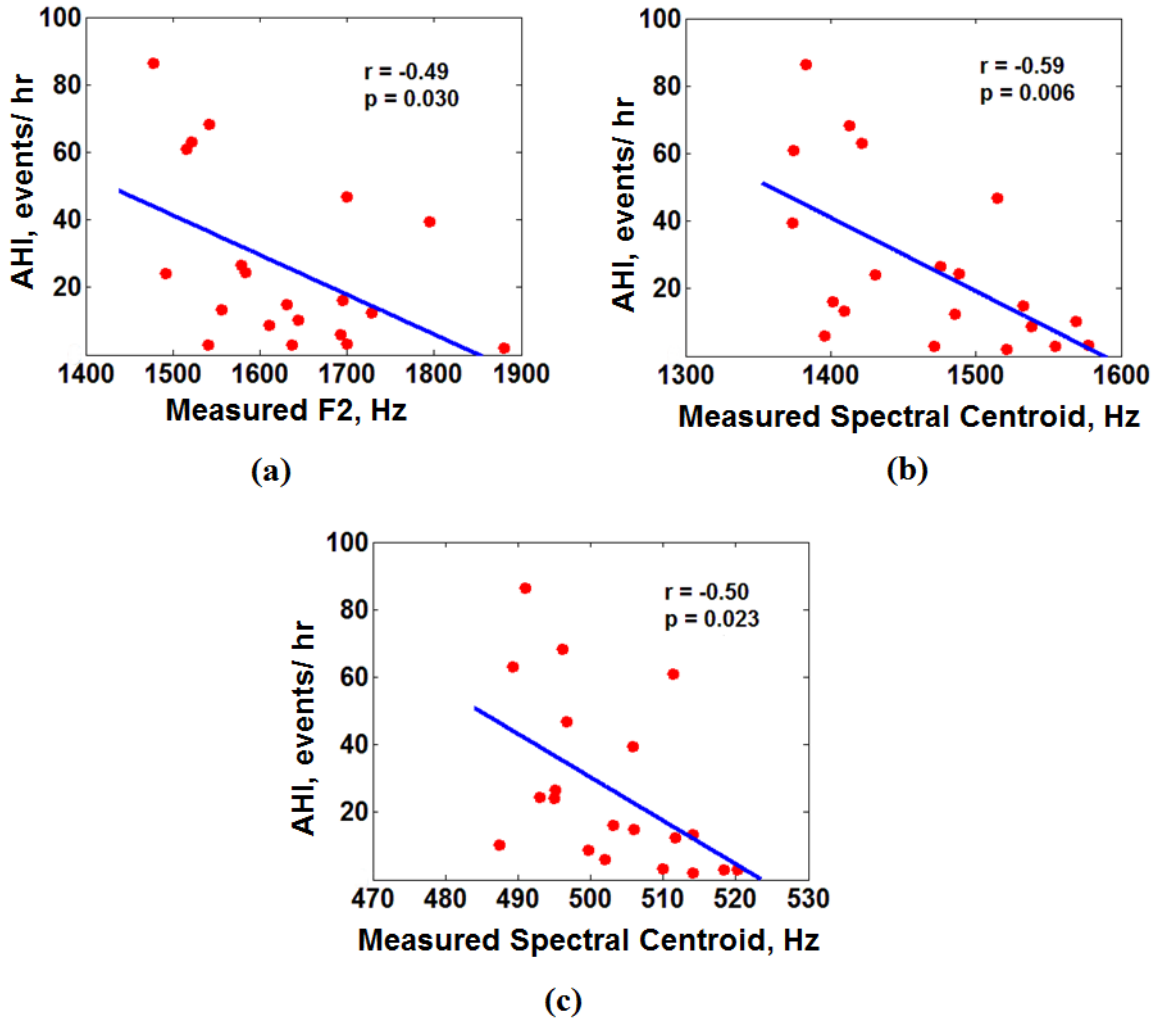

Figure 2.5: Relationship between AHI and measured snoring sounds frequencies (assessed by Pearson Correlation Coefficient): (a) Decreases in F2 were significantly correlated with the increases of AHI; (b) Decreases in spectral centroid of snoring sounds (calculated over the entire sleep duration) within 1200-1800 Hz frequency range were significantly correlated with the increases of AHI; (c) Decreases in spectral centroid of snoring sounds (calculated over the entire sleep duration) within 450-600 Hz frequency range were significantly correlated with the increases of AHI.

2.2.5 Effects of upper airway anatomy on the intensity of snoring sounds

We calculated the effects of changes in UA-XSA, UA-Length, and airway wall thickness on the snoring sounds intensity.

2.2.5.1 Results obtained from the modeled snoring intensity

There was a significant correlation between percentage narrowing in the UA-XSA from before to after sleep and the gain of the upper airway model (Fig. 2.6-a, $r=-1.00$, $p<0.001$); indicating that upper airway narrowing increases the modeled intensity of snoring. On the other hand, there were no significant correlations between the gain of the upper airway model and changes in wall thickness or UA-Length ($p>0.10$ for both).

2.2.5.2 Results obtained from measured snoring intensity

There was a significant correlation between the measured average intensity (average power of recorded snoring sounds in 100-4000Hz) of all snoring segments during sleep and the percentage narrowing of UA-XSA from before to after sleep (Fig. 2.6-b, $r=-0.53$, $p=0.018$). Moreover, for each subject, we calculated the average intensity of 5 snoring segments in the first and last 15 minutes of N2 sleep. The results showed that from the first to the last part of N2 sleep, there was a significant increase in the measured intensity (Fig. 2.6-c, $\Delta=2.0\pm3.8$ dB). These were similar to those based on the simulation ($p=0.947$). On the other hand, there were no significant correlations between the measured intensity of recorded snoring sounds and changes in the upper airway wall thickness or UA-Length ($p>0.1$ for both).

Therefore, both modelling and measured results suggested that there was an inverse relationship between the snoring intensity and UA-XSA.

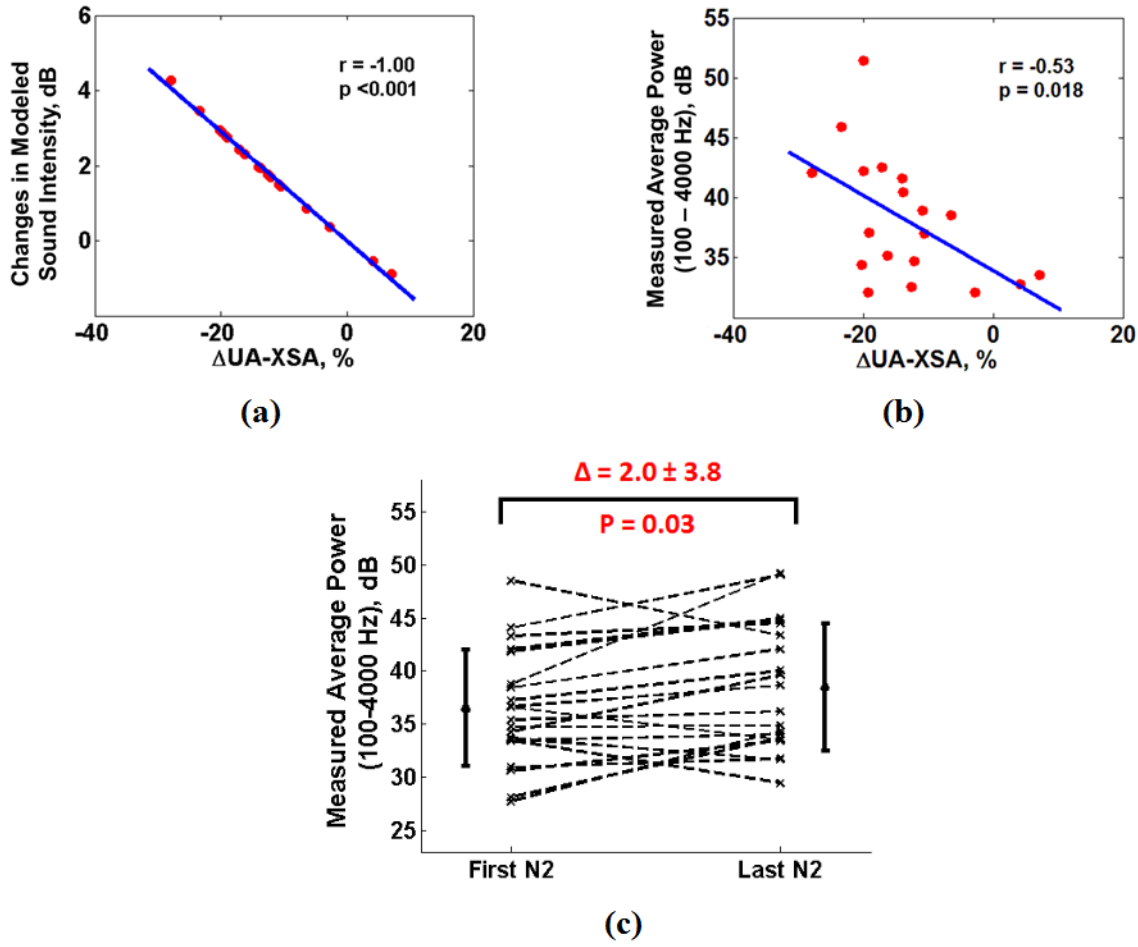

Figure 2.6: Relationship between changes in upper airway cross sectional area during sleep and snoring sounds intensity (assessed by Pearson Correlation Coefficients): a) Result obtained from the modeled snoring intensity: narrowing in the UA-XSA was strongly correlated with increases in the intensity of the sounds; b) Result obtained from the measured snoring intensity: narrowing in the UA-XSA during sleep was significantly correlated with increases in the average power of snoring sounds (calculated over the entire sleep duration) within 100-4000 Hz frequency range; c) Results obtained from the measured snoring intensity: There were significant increases in the average power snoring sounds from first part to the last part of the N2 sleep stage (assessed by paired t-test).

2.3 Discussion

To the best of our knowledge, this is the first study to develop a subject-specific model of the upper airway and to consider the fact that changing in the upper airway area could also change other anatomical factors of the upper airway such as wall thickness. Our model showed that the upper airway narrowing during sleep increases snoring intensity, while increases in the UA-Length reduced the resonant frequency of snoring. The model was validated against recordings of actual snoring. Furthermore, we found that measured resonant frequencies of snoring were inversely related to the OSA severity.

Our proposed model for the snoring sounds generation included snoring source vibration and propagation of the vibrations through the upper airway. A novelty of this study was that we modeled the snoring source as a single frequency vibratory signal due to either soft palate vibration or pharyngeal tissue vibration at the site of upper airway narrowing. Similar to speech articulation[59], we considered the measured pitch frequency of snoring sounds as the main vibrating frequency of snoring source[51]. We found the measured pitch frequency of the recorded snoring sounds were less than 150 Hz. Previous studies in dog models for inducing snoring sounds have shown that the main frequency of snoring was in the range of 64-135 Hz [65]. Although, dog models are not true representatives of human upper airway, these results support our assumption that pitch frequency can represent the main vibratory source of snoring sounds. As part of having a subject-specific model, for every individual we used the measured pitch frequency of his recorded snoring to characterize the snoring sounds source.

An important finding of this study was that narrowing of the upper airway during sleep may increase the turbulent airflow and increase the snoring sounds power. On the other hand, narrowing in the upper airway can increase sleep apnea severity[66]. Our results showed a

positive correlation between AHI and measured relative power of snoring sounds. These results are consistent with those of Maimon et al. who showed that snoring sounds intensity is related to severity of OSA[18].

Another major finding of our model was that modeled resonant frequency of snoring was inversely related to the upper airway length. Conversely, there was an inverse relationship between OSA severity and measured resonant frequency of snoring sounds. Imaging and cephalometric studies have shown that patients with OSA have longer upper airway than those without OSA [1, 62, 63]. Similarly, previous studies have shown that in vowel articulation, formant frequencies for articulating /i/ or /u/ (e.g. in “see” or “moo”) are significantly lower in patients with OSA than non-OSA individuals[67, 68]. Although, snoring sounds and speech have different vibratory sources, the role of upper airway in generating sounds may be similar for both signals. Therefore, these results may provide proof of concept for the potential applications of resonant frequencies of snoring sounds to assess the effects of upper airway length on OSA severity.

Previous studies have shown that the main frequencies of the snoring sounds vary depending on the site of obstruction [69, 70]. While the main frequencies of snoring due to the narrowing at the base of tongue were above 650 Hz, frequencies of palatal snoring were below 450 Hz [69, 70]. In this study, we did not have any measurement to assess the site of upper airway obstruction. However, if we assume that the length of upper airway in our model represents the distance between the site of obstruction and the recording microphone, the resonant frequency of simulated palatal snoring was 450 Hz; while it was approximately 800 Hz for the snoring originating closer to the glottis. These simulation results, which should be verified in future

studies, may provide non-invasive techniques to assess the site of upper airway obstruction in snorers and patients with OSA.

Our study was subject to some limitations. Since daytime sleep studies were performed, these results may not be the same as those during nocturnal sleep. Furthermore, we modeled the snoring sounds generation and propagation using a single segment tube model. Further studies will be needed to develop a multi-segment tubular model to include the effects of oral and nasal cavities on snoring sounds features. Also, participants in this study were non-obese men. Future research will need to examine snoring features and upper airway properties in other populations such as obese individuals, women, and children. Furthermore, we limited the participants to supine sleep. Therefore, our results may not be fully applicable to other sleeping postures.

In conclusion, this study attempted to develop an acoustic model of the upper airway for snoring sounds generation and to investigate the effects of changes in upper airway narrowing and length on snoring sounds features. Future studies should validate the proposed model based on simultaneous recordings of snoring sounds, UA-XSA and sites of collapse during sleep. Since snoring sounds can be recorded non-invasively and conveniently during multiple nights; once validated, the proposed model can be used to assess the dynamics of upper airway narrowing during sleep.

2.4 Methods

2.4.1 Participants

Healthy non-obese and normotensive men were recruited by advertisement and participated in this study [46]. Individuals with a history of cardiovascular, respiratory, renal, or neurological

diseases, or previously diagnosed of OSA, or those who slept less than one hour during the protocol, or with central dominant sleep apnea were excluded from the study.

2.4.2 Experimental protocol

Participants arrived in the sleep laboratory at early afternoon after a night of voluntary sleep deprivation and were instrumented for sleep studies. Baseline measurements including UA-XSA, UA-Length, and NC were performed in supine position before sleep and just after the participants woke up (see Appendix D). Breath and snoring sounds were recorded continuously and simultaneously with polysomnography during sleep [46].

The experimental protocol was approved by the Research Ethics Board of Toronto Rehabilitation Institute-University Health Network and all participants signed written consent prior to participation [46]. The study was performed in accordance with the approved guidelines and regulations.

2.4.3 Data measurement

2.4.3.1 Sleep studies

Daytime polysomnography was performed for the convenience of participants and the research personnel. Thoracoabdominal motion, nasal pressure, and arterial oxyhemoglobin saturation (SaO_2) were monitored by respiratory inductance plethysmography, nasal cannulae, and oximetry, respectively [71] . Scoring sleep stages and arousals were done by a specialist using standard techniques and criteria. The definition and classification of apneas (cessation of airflow to the lungs for at least 10s) and hypopneas (>50% decrease in breathing airflow for more than 10s with blood oxygen desaturation of >3%) were done in accordance the American Academy of Sleep Medicine (AASM) [72]. To minimize any possible effect of postural changes on AHI and

other variables, participants slept supine on a single pillow for the entire study duration. Sleep studies were scored by personnel blind to the fluid measurements and vice versa [46].

2.4.3.2 UA-XSA, UA-Length and NC measurement:

UA-XSA and UA-Length (the distance from velum to glottis) were measured by acoustic pharyngometry [73]. NC was assessed by a measuring tape. A line was drawn just above the cricothyroid cartilage to ensure the measurements before after sleep were made at the same level.

2.4.3.3 Breath and snoring sounds recoding

Breaths along with snoring sounds were recorded by a Sony EMC-44B omni-directional microphone. The microphone was placed over suprasternal notch using double-sided adhesive tape. The sounds were filtered by a low-pass filter (cut off frequency of 5 kHz) using Biopac DA100C, and digitized at sampling rate of 12.5 kHz using MP150 Biopac System [74].

2.4.4 Data analysis

After manual segmentation of snoring sounds, several features in the temporal and spectral domains were extracted.

2.4.4.1 Temporal Feature

- Snoring Time Index: Total snoring time in each sleep stage divided by the time spent in each sleep stage.

2.4.4.2 Spectral Features

Snoring segments were band-pass filtered in the frequency range of 100-4000 Hz to remove the effects of heart sounds in low frequency ranges as well as high frequency noises[57]. Power spectral density (PSD) of each snoring segment was calculated based on the Welch method with

a Hamming window of 100 ms and 50% overlap between adjacent windows. Based on the PSD, following features were calculated:

- Average Power: Average power of the snoring sounds in eight frequency bands of 100-4000 Hz, 100-150 Hz, 150-450 Hz, 450-600 Hz, 600-1200 Hz, 1200-1800 Hz, 1800-2500 Hz, and 2500-4000 Hz were calculated [75] (See Appendix A).
- Relative Power: The average power of snoring sounds in each sub-band divided by the average power in entire frequency band (100-4000 Hz).
- Spectral Centroid: It represents the frequency that contains the maximum power of snoring sounds in any of the eight frequency bands [76].

$$\text{Spectral Centroid} = \frac{\sum_{f_l \le f \le f_u} fP(f)\Delta f}{P_{avg}(f_l \le f \le f_u)} \quad (2.1)$$

  Here, P_{avg}= Average power; f_l = Lower band frequency; f_u = Higher band frequency; $P(f)$ = Estimated power spectral density.

- Pitch and Formant Frequencies: Pitch frequency was calculated based on the robust algorithm for pitch tracking[77]. For calculating formants, snoring segments were pre-processed using a Hamming window (window size of 20 ms) and a pre-emphasizing filter. Then, 16th order linear predictive coding (LPC) spectrum of the snoring sounds was estimated to extract formants [78, 79]. Pitch was calculated using the validated "Voicebox" toolbox[80].

2.4.5 Modelling of the upper airway for snoring sounds generation and propagation

We proposed a simplified two-compartmental model for snoring sounds generation that included snoring source vibration and the upper airway response as a collapsible tube (Fig. 2.3).

2.4.5.1 Snoring source vibration

Snoring sounds can be generated either by oscillation of the soft palate or the upper airway wall [14]. Based on the Bernoulli's theorem, in a collapsible tube such as the upper airway, upper airway narrowing or increased negative intra-thoracic pressure during inspiration increases the airflow speed which will cause a pressure drop across the upper airway; this sequence of events will further increase the negative pressure in the upper airway, narrow the upper airway and increase the airflow speed[14]. The consequence of these events is an increase in turbulence of airflow within the upper airway, which leads to vibration of soft palate or the airway wall tissue and induces snoring sounds[14]. Considering speech articulation, vibration of soft palate or the upper airway wall during snoring sounds generation can be assumed to be analogous to the vibration of vocal cord[51]. Therefore, we assumed that pitch frequency represent the fundamental frequency of snoring sounds. Thus, we modeled the snoring sounds source (Fig. 2.3) as a sinusoid signal with its frequency equal to the pitch of the recorded snoring sounds for every individual subject.

2.4.5.2 Subject-specific upper airway model

The upper airway was modeled as a collapsible tube [27, 60, 61, 81, 82]. In this model, the air pressure and airflow were modeled as the voltage and current, respectively. The model included acoustic resistance of airflow (R_a), compliance (C_a), inertance (L_a), and conductance (G_a)[81, 82]; as well as upper airway wall resistance (R_w), inertance (L_w) and compliance (C_w)[60, 61, 83]. Detailed definitions of the model variables are presented in the Appendix B. In this study, we used the previously reported measurements for the air and tissue properties such as viscosity and elasticity [27, 60, 81, 82, 84, 85] (See Appendix B). Previous models of the upper airway did not incorporate the differences in the upper airway anatomy among subjects such as its internal

radius and wall thickness. For each subject, we used measurements of UA-XSA and NC to estimate the upper airway wall thickness (Fig. 2.3). Upper airway radius (T_r) was calculated as square root of (UA-XSA/π), neck radius (N_r) was estimated as (NC/2π), and the upper airway wall thickness (h) was calculated as (N_r - T_r).

2.4.6 Statistical analysis

The changes in NC, airway wall thickness, and UA-XSA from before to after sleep were assessed by paired t-tests for normally distributed data and Wilcoxon rank-sum test for non-normally distributed data. Paired t-tests were performed to investigate the differences between the measured average powers of recorded snoring sounds from the beginning to the end of sleep. The changes in measured snoring sounds features between different sleep stages were investigated by analysis of variance (ANOVA) and the post-hoc Tukey test. All the correlation analyses were performed based on Pearson or Spearman's rank coefficient, for normally and non-normally distributed data, respectively. Furthermore, we performed Bland-Altman statistical test to verify the agreement between modeled and measured resonant frequencies. Statistical analyses were performed by Matlab and two-tailed $P<0.05$ was considered as significant. Data are presented as mean±SD.

Chapter 3

3 Effects of Fluid Accumulation in the Neck on Features of Snoring Sounds

The content of this chapter is going to be submitted in a peer reviewed journal article Shumit Saha, Zahra Moussavi, Peyman Hadi, T. Douglas Bradley, Azadeh Yadollahi, *Effects of Fluid Accumulation in the Neck on the Acoustic Features of Snoring Sounds*.

Except for the formatting and some organizational and stylistic improvements, the content of this chapter is almost identical to the submitting journal article. Contribution of authors is as follows: Shumit Saha manually annotated the snoring segments from breath sounds, performed the signal processing, statistical analysis and proposed a spring and mass model for the pharyngeal tissues of the upper airway. Azadeh Yadollahi and Zahra Moussavi supervised all the aspects of this work and edited and reviewed the paper. T Douglas Bradley and Azadeh Yadollahi designed the experimental protocol and acquired all the physiological data. Peyman Hadi helped in the development of the spring and mass model.

This chapter demonstrates the effects of fluid accumulation in the neck on the acoustic features of snoring sounds.

3.1 Introduction

Obstructive sleep apnea (OSA), a common respiratory disorder, is highly associated with the chronic diseases like stroke [3], heart failure [4, 5], as well as car and work related accidents [6-8]. OSA occurs due to the partial (hypopnea) or complete (apnea) cession of breathing due to either partial or complete collapse of the upper airway during sleep [1]. The Upper airway

collapse during sleep is multi-factorial [11], and the exact underlying mechanisms of upper airway narrowing are still unknown. Previous studies have shown that increased tissue content in the neck, either by the increased pharyngeal fat or edema, contribute to the upper airway narrowing, and increase its resistance, collapsibility and worsening of the OSA severity [86, 87]. Furthermore, rostral fluid shift from the legs into the neck during sleep can increase the neck fluid volume (NFV), and further increase the pharyngeal tissue edema [88]. Therefore, developing convenient and non-invasive techniques to measure the increased tissue edema and monitoring its effects on the upper airway narrowing could improve OSA management.

Previous studies have demonstrated that due to gravity, lack of activity and the sedentary lifestyle fluids are accumulated in the legs during daytime [56]. When lying down at night, the fluid would be shifted from the legs into the upper body parts (i.e. abdomen, thorax and neck) [89]. The rostral fluid shift to the neck during sleep increases the NFV. Consequently, the increases in NFV could narrow upper airway cross sectional area (UA-XSA) [90], and increase the upper airway resistance [12] and collapsibility [13]. Furthermore, previous studies showed that in older men (>40 yr old) with mild to moderate OSA, increases of fluid in their vein by injecting normal saline resulted in three-fold increment in their apnea/hypopnea index (AHI) [46]. Conversely, in patients with chronic venous insufficiency, one week wearing of the compression stockings caused 30% reduction in the AHI [38, 91]. These results proved the concept that fluid accumulation in the neck during sleep can change the properties of the upper airway and increase the risk of developing OSA.

The gold standard methods to measure the NFV are based on MRI or bioelectrical impedance which are inconvenient and difficult to perform continuously during sleep. On the other hand,

respiratory or snoring sounds analysis is a simple and non-invasive method to investigate variations in the upper airway anatomy and monitor upper airway obstruction during sleep [29, 50]. Turbulence of the air flowing through the upper airway and vibrations of the pharyngeal tissues due to the narrowing of the upper airway contribute to the generation of snoring sounds [14]. These vibrations are transmitted through the pharyngeal tissue, and can be recorded by a microphone placed over the neck. Thus, acoustic features of the snoring sounds can change not only with the anatomy of the upper airway but also with the tissue composition of the upper airway. Although snoring sounds analysis have been used to monitor the upper airway narrowing [50] or site of obstruction [92], its relationship with changes in tissue edema and NFV during sleep has not been investigated before.

Previously, we showed that tracheal respiratory sounds could be used to detect the amount of NFV in healthy subjects while awake [74]. Furthermore, we showed that snoring sounds features, such as its intensity or formant frequencies can represent narrowing in the upper airway [50], and OSA severity [16, 93]. These studies provide a strong proof of concept that snoring sound analysis could represent variations in the upper airway due to edema and NFV during sleep.

This study aims to investigate the effects of fluid accumulation in the neck during sleep on the acoustic features of snoring sounds. Based on the physics of the sound propagation through a tissue, we hypothesize that fluid accumulation in the neck during sleep will change the spectral frequencies of the snoring sounds. We have developed a spring and mass model for the pharyngeal tissue surrounding the upper airway, and investigated the effects of pharyngeal tissue and increased NFV on snoring sounds features.

3.2 Method

3.2.1 Data Measurement

3.2.1.1 Experimental protocol, participants and sleep studies

This study was part of a randomized, double cross-over study to investigate the effects of fluid overloading by saline infusion on sleep apnea severity in men [46]. The study was approved by the research ethics board of the University Health Network and all participants gave written consent before participation in the study. Daytime polysomnography was performed, and subjects slept in supine position only on a single pillow. Polysomnography (PSG) was used to detect sleep stages and sleep apnea severity assessed by apnea-hypopnea index (AHI). Details of the experimental protocol and sleep studies are similar to those of our previous study elaborated in [46, 50] (see Appendix D).

3.2.1.2 NC, UA-XSA and NFV measurement

NC and UA-XSA were measured before and after sleep using a measuring tape and acoustic pharyngometry, respectively. In this study, NFV was estimated based on the bioelectrical impedance measurement of the neck. It is based on the fact that tissue impedance is inversely related to the fluid content of the tissue. The following equation was used to estimate NFV (see Appendix C):

$$V = \left(\frac{\rho^2 L^5 C^2}{4\pi R^2}\right)^{1/3}, \qquad (3.1)$$

where C is the neck circumference, L is the neck length, R is the neck resistance estimated from the bioimpedance measurement (using MP150 Biopac System and EBI100C module), and ρ is the fluid resistivity. To measure bioimpedance, two electrodes were placed on the right side of the neck below the right ear and at the base of the neck to measure the voltage drop across the

length of the neck. Two other electrodes were placed one inch from the voltage measuring electrodes to inject a low amplitude (400μA) current at 50 kHz. At the beginning of the study, the neck length (L in Equation 1) was measured with a tape as the distance between the voltage measuring electrodes, while the subjects were standing and their head was in the neutral position. Details of this method are discussed in [94].

3.2.1.3 Breath and snoring sounds recording

During sleep, breathing and snoring sounds were recorded with a Sony EMC-44B omni-directional microphone placed over suprasternal notch. The sounds were low-pass filtered (cut off frequency of 5 kHz) and digitized (sampling rate of 12.5 kHz) by Biopac DA100C and MP150 Biopac System, respectively.

3.2.2 Feature extraction

From the breathings sounds recording during sleep, snoring segments were manually extracted. Manual annotation of snoring sounds were done by listening to the sounds along with simultaneous visual inspection of the spectrogram of each segment using a digital audio software called Praat (Version 5.4.08) [95] (Figure 3.1). Since snoring during inspiratory phase is more common than snoring during expiratory phase, we only investigated the inspiratory snoring segments. After manual segmentation of snoring sounds, different features in the time and frequency domains were extracted.

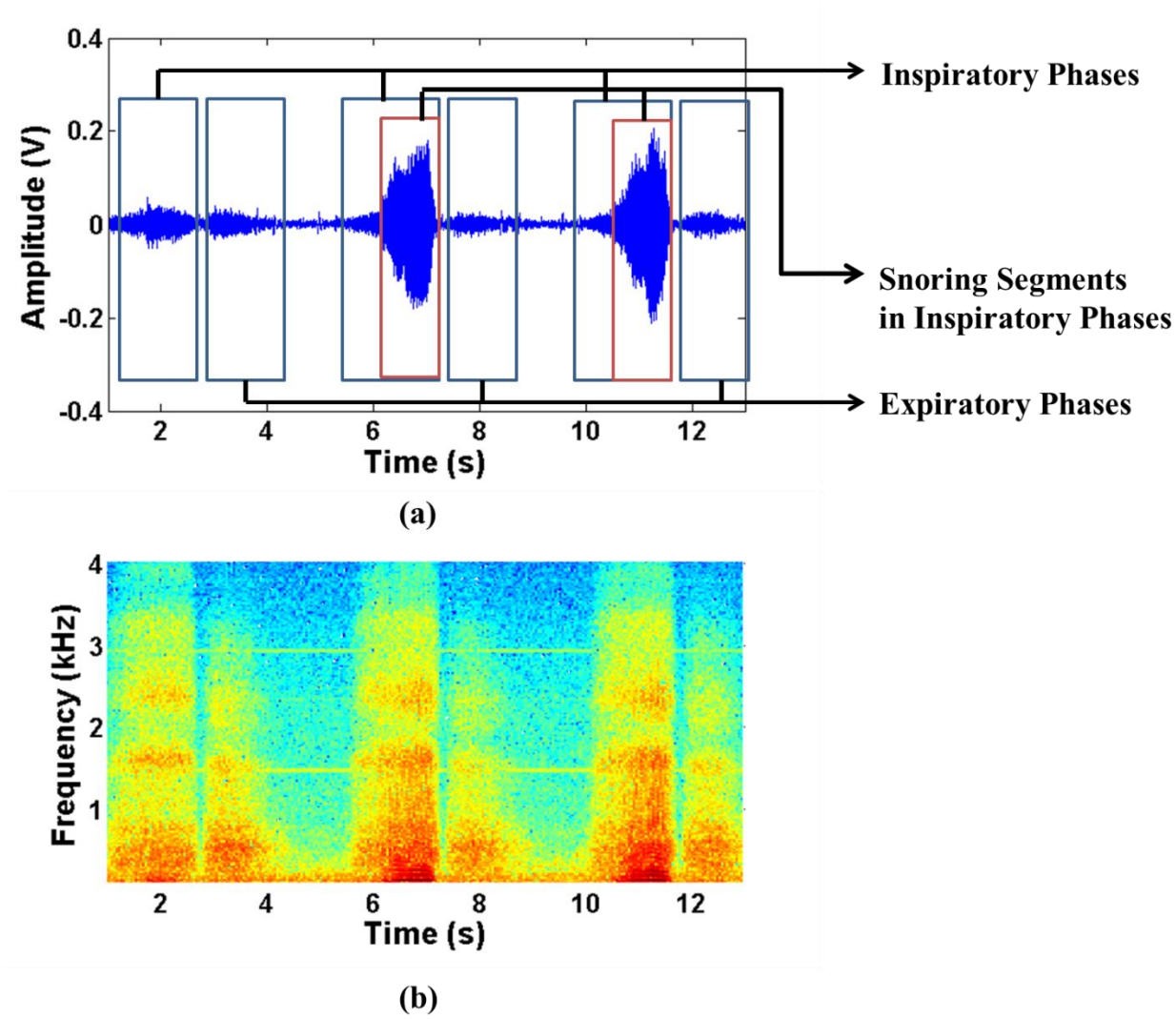

Figure 3.1: Segmentation of snoring sounds: a) 13 sec. breathing segments with normal inspiratory phases, expiratory phases and snoring sounds segments; b) Spectrogram of the breath segment presented in (a). Inspiratory phases show larger intensity in spectrogram than expiratory phases. Furthermore, snoring sounds intensity was larger than those of the inspiratory and expiratory breath sounds without snoring.

In time domain, we calculated two features: snoring percentage and snoring time index. Snoring percentage was calculated as the number of snoring segments in each sleep stage divided by the total number of snoring segments in the entire sleep. Snoring time index was calculated for the total sleep and individual sleep stages. Snoring time index for total sleep time was calculated as the total snoring duration during the entire sleep divided by the total sleeping time. Furthermore, snoring time index in each sleep stages was calculated as the total snoring time in each sleep stage divided by the time spent in that sleep stage.

To calculate the spectral features, snoring segments were band-pass filtered in the frequency range of 30-4000 Hz to remove the effects of heart sounds in low frequency ranges as well as high frequency noises [57]. We estimated power spectral density (PSD) of each snoring segment based on the Welch method using a Hamming window of 100 ms and 50% overlap between adjacent windows. From the PSD, we calculated the average power and spectral centroid of all snoring segments. Average power, calculated from the PSD of the sound signal, represents the intensity of the snoring sounds. Spectral centroid represents the weighted average of the PSD frequencies within a frequency band [76]. The equations of average power and spectral centroid are given below:

$$\text{Average Power, } P_{avg}\left(f_l \le f \le f_u\right) = \sum_{f_l \le f \le f_u} P(f)\Delta f \quad , \tag{3.2}$$

$$\text{Spectral Centroid} = \frac{\sum_{f_l \le f \le f_u} f \times P(f)\Delta f}{P_{avg}\left(f_l \le f \le f_u\right)} \quad , \tag{3.3}$$

where, P_{avg} = Average power, f_l = Lower band frequency, f_u = Higher band frequency, and $P(f)$ = Estimated power spectral density.

Both the average power and spectral centroid were calculated for the entire frequency band (30-4000 Hz). In addition, spectral centroid was calculated for several sub-bands including 60-140 Hz, 60-170 Hz, 60-200 Hz, 100-150 Hz, 150-450 Hz, 450-600 Hz, 600-1200 Hz, 1200-1800 Hz, 1800-2500 Hz, and 2500-4000 Hz [50, 75]. Previous studies have shown that the main vibratory frequency of the snoring sounds lies in 64-135 Hz [65]; therefore, we choose sub-bands more densely in the lower frequency ranges. Next, for each subject, we calculated the average of spectral centroid and P_{avg} for all the snoring segments during the entire sleep and also for each sleep stage separately. Then, we investigated the relationship of these average values with the changes in NFV and NC in every subject.

We further investigated the changes in spectral centroid over the sleep time for each subject. To accomplish this task, we calculated the average spectral centroid of 5 snoring segments in the first and last 30 minutes of stage 2 of sleep void of apneas and hypopneas, calculated its difference between the two periods of sleep, and investigated its relationship with changes in NC and NFV.

3.2.3 Spring and mass model for the surrounding tissues of the upper airway

If a force is applied to a system that consists of a mass (m) attached to a spring with elasticity (K), the mass exhibits a simple harmonic motion, with the natural frequency of $f = \frac{1}{2\pi}\sqrt{\frac{K}{m}}$ [96]. Therefore, the natural frequency of a system depends on its elasticity and mass. In this study, pharyngeal tissue around the upper airway was modeled as a mass and spring system (Figure 3.2), where K and m were the elasticity and mass of the surrounding tissues of the upper airway, respectively. The mass of the surrounding tissues of the upper airway was calculated from the density (d) and volume of the tissue (V):

$$m = d \times V. \tag{3.4}$$

Therefore, the frequency of the tissue vibration due to snoring sounds propagation was derived as:

$$f = \frac{1}{2\pi}\sqrt{\frac{K}{d \times V}}\ , \tag{3.5}$$

where, V represents the total volume of the surrounding tissues of the upper airway including all the fat, fibers, muscles, fluids, etc. In this study, we assumed that from beginning to the end of sleep, the only factor that would change the tissue volume surrounding the upper airway is the changes in NFV. Therefore, Eq. 3.4 could be rewritten as:

$$\Delta f = \frac{1}{2\pi}\sqrt{\frac{K}{d \times \Delta V}} \tag{3.6}$$

where, Δf and ΔV are the changes in snoring sounds frequency and changes in tissue volume due to NFV from beginning to the end of sleep. Previous studies have shown that with the changes in water content, there's a negligible change in the elasticity of the body-fat [97]. Therefore, we assumed that increased NFV did not change the elasticity of the tissue in Eq. 3.6.

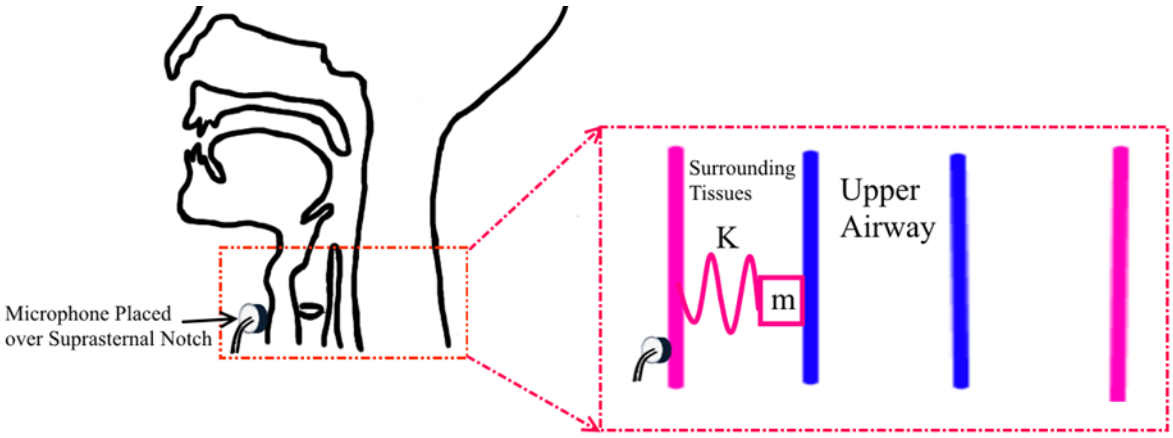

Figure 3.2: The spring and mass system of surrounding tissues of upper airway. Here, K: the elasticity of the tissue and m: the mass of the tissue

3.2.4 Statistical analysis

The changes in NC, UA-XSA, and NFV from before to after sleep along with the changes in spectral centroid from beginning to the end of sleep were assessed by paired t-tests or Wilcoxon rank-sum test for normally and non-normally distributed data, respectively. Correlations between the snoring sounds features and changes in the NFV and NC were investigated by Pearson or Spearman's rank coefficient, for normally and non-normally distributed data, respectively. Correlations between spectral centroid change from first to end of the sleep and changes in NFV or NC from before to after sleep were also performed by Pearson or Spearman's coefficient based on their normality. Statistical analyses were performed by Matlab and two-tailed $p<0.05$ was considered as significant. Data are presented as mean ± STD.

3.3 Results

Twenty men met all inclusion criteria and were included in this study. Participants slept for an average of 150 minutes (Table 3.1) and 14 out of 20 men had at least one full sleep cycle; including both rapid eye movement (REM) and non-REM sleep stages. Furthermore, participants spent maximum time in stage 2 of the non-REM sleep (Table 3.1). From before to after sleep, there were significant increases in NC (ΔNC: 0.5±0.3cm, $p<0.001$) and NFV (ΔNFV: 18.6±6.9ml, $p<0.001$) and decreases in UA-XSA (ΔUA-XSA: -0.4±0.3cm^2, $p<0.001$).

Table 3.1: Characteristics of the participants (n = 20)

Baseline Characteristics		**Sleep Structure**	
Variable	**Mean ± STD**	**Variable**	**Mean ± STD**
Age, years	45.1 ± 11.4	Total sleep time, min	150.1 ± 46.1
Height, cm	176.9 ± 6.3	Non-Rem 1 sleep, %	18.0 ± 10.4
Weight, kg	79.0 ± 10.7	Non-Rem 2 sleep, %	57.2 ± 15.1
BMI, kg/m^2	25.4 ± 3.05	Non-Rem 3 sleep, %	11.5 ± 12.9
NC , cm	41.8 ± 2.9	REM sleep, %	10.7 ± 8.1
UA-XSA, cm^2	2.6 ± 0.6	Sleep efficiency, %	74.7 ± 15.0
NFV, ml	265.7 ± 49.5	AHI, /h	27.6 ±25.8

An average of 342 ± 223 inspiratory snoring segments was manually extracted from the entire sleep for every individual (134.2 ± 96.0 snoring segments per hour of sleep). The number of snoring segments in stage 2 was significantly higher than that in other sleep stages ($p<0.001$). However, the snoring time index was similar for different sleep stages ($p>0.10$). Similarly, snoring time index was similar in both non-REM sleep and REM sleep ($p>0.10$). Furthermore, no significant correlation between the time domain features of snoring sounds and NFV.

We found a significant and negative correlation between the increases in NFV during sleep and the spectral centroid of snoring sounds in the frequency range of 100-150 Hz (Figure 3.3-a, r=-0.47, p=0.037) for the entire duration of sleep. Similar correlations were found between ΔNFV and spectral centroids of snoring sounds during stage 2 (r=-0.51, p=0.031) and stage 3 (r=-0.52, p=0.054) of sleep. We also found that increases in NFV during sleep were significantly correlated with the decreases in spectral centroid of snoring sounds in the frequency range of 60-170 Hz (r =-0.46, p=0.048) and 60-200 Hz (Fig. 3.3-b, r =-0.50, p=0.026) for stage 2 of sleep. However, we found no significant correlation between ΔNFV and spectral centroid when calculated in higher frequency ranges. Furthermore, we found that the percentage increase in NC during sleep was significantly correlated with the reduction in spectral centroid in 60-140 Hz (r=-0.57, p=0.008), 60-170 Hz (Fig. 3.3-c, r=-0.57, p=0.009) and 60-200 Hz (Fig. 3.3-d, r=-0.53, p=0.016) for stage 2 of sleep.

As shown in Fig. 3.4, the spectral centroid of snoring sounds changed significantly from the first to the last part of sleep: 60-170 Hz (Fig. 3.4-a, p=0.039, Δ = -5.8 ± 11.7 Hz), and 60-200 Hz (Fig. 3.4-b, p=0.010, Δ = -9.8 ± 14.1 Hz).

There was a borderline significance between decreases in the spectral-centroid change in 60-170 Hz with the percentage increases in the ΔNC from before to after sleep (Fig. 3.5-a, r=-0.44, p=0.053). Although, there was a trend for an inverse relationship between changes in the spectral-centroid calculated over the entire band (30-4000 Hz) and the changes in NFV from before to after sleep (Fig. 3.5-b, r=-0.39, p=0.088). No significant correlations were found between ΔNFV and P_{avg} of snoring sounds.

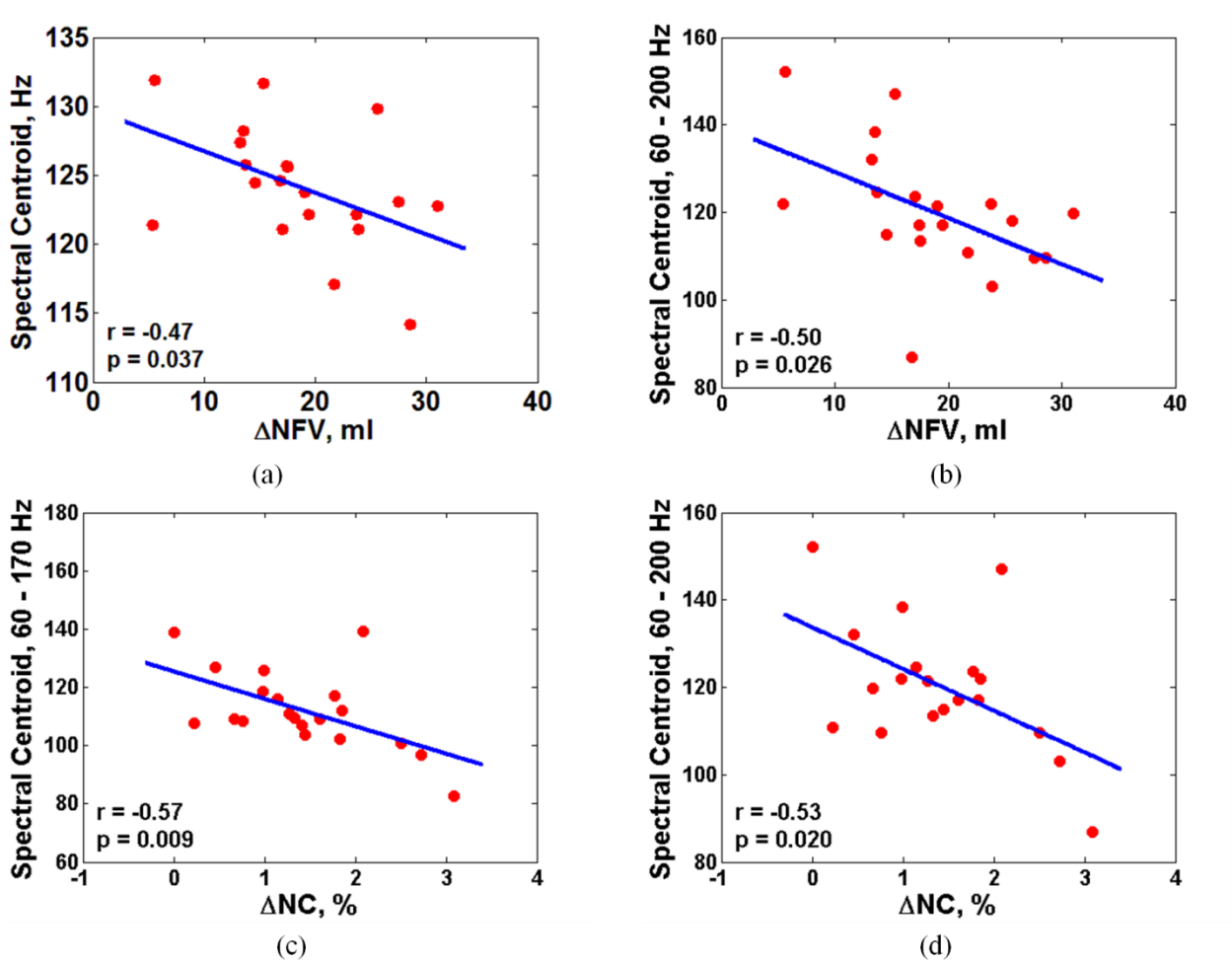

Figure 3.3: a) Relationship between changes in NFV during sleep and spectral centroid of snoring sounds (calculated over the entire sleep duration) within 100-150 Hz frequency range; b) Relationship between changes in NFV and spectral centroid of snoring sounds (calculated over the non-Rem 2 (N2) sleep stage duration) within 60-200 Hz frequency range; c) Relationship between changes in percentage NC and spectral centroid of snoring sounds (calculated over the N2 sleep stage duration) within 60-170 Hz frequency range; d) Relationship between changes in percentage NC and spectral centroid of snoring sounds (calculated over the N2 sleep stage duration) within 60-200 Hz frequency range.

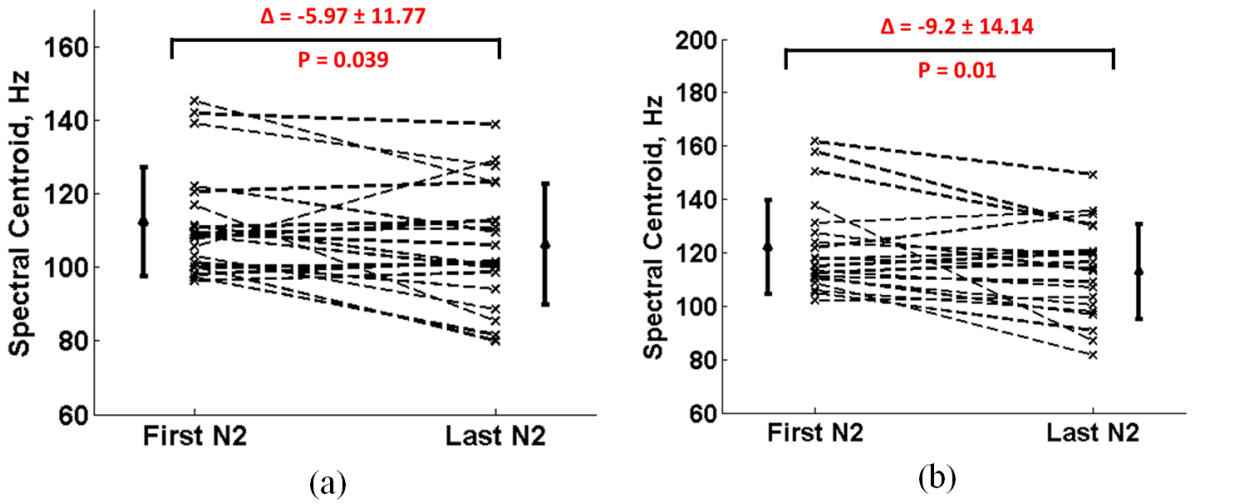

Figure 3.4: a) There were significant decreases in the spectral centroid snoring sounds from first part to the last part of the N2 sleep stage in 60-170 Hz frequency range; b) There were significant decreases in the spectral centroid snoring sounds from first part to the last part of the N2 sleep stage in 60-200 Hz frequency range (assessed by paired t-test).

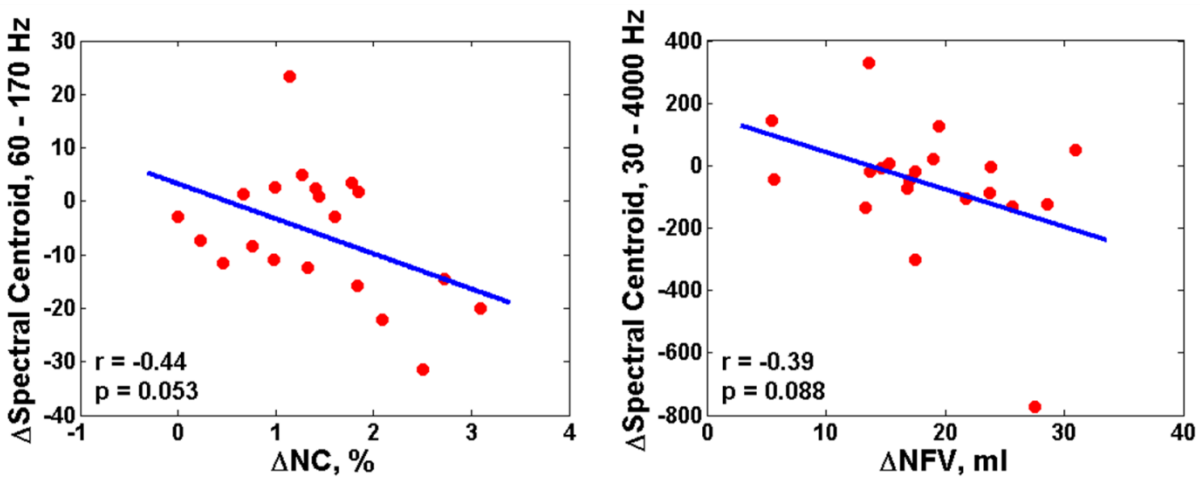

Figure 3.5: a) Relationship between the spectral-centroid change and ΔNC in 60-170 Hz frequency band; b) Relationship between the spectral-centroid change and ΔNFV in 30-4000 Hz frequency band.

3.4 Discussion

To the best to our knowledge, this is the first study which investigated the relationship between fluid accumulation in the neck during sleep and snoring sounds features. The most important findings of this study were that increases in NFV during sleep were significantly correlated with the decreases in spectral centroid in the frequency range of 60-170 Hz, 60-200 Hz in stage 2 of sleep and 100-150 Hz in entire sleep duration. Furthermore, there were no correlations between changes in NFV and snoring sounds features in the higher frequency ranges. Previous study have shown that the low frequency components (< 600 Hz) of breath sounds tend to couple with the tissue filled compartment and propagate through the tissue [78]. However, the high frequency components tend to propagate through the airway path rather than tissue because the airway walls behave as rigid structures at higher frequencies [78]. Therefore, it is justified that lower frequency components of snoring sounds might be affected by the fluid accumulation in the neck and not the higher frequency components.

We found that the increases in NFV during sleep were significantly correlated with the decreases of the spectral centroid of the snoring sounds. This was further supported by the Eq. 3.6 of the spring and mass model described in the methods section. Increases in NFV could increase the mass of the surrounding tissues of the upper airway and consequently decrease the centroid frequency. These results were further supported by the strong inverse correlation between ΔNC during sleep and decreases in spectral centroid. We acknowledge the fact that this analysis is based on the assumption that increases in NFV do not change the pharyngeal tissue elasticity. Future studies are required to measure the stiffness of the pharyngeal tissue and its association with NFV.

Since NFV change continuously while supine [94], it is expected that centroid frequencies of snoring sounds would change from beginning to the end of sleep. Our results showed that from beginning to the end of sleep, spectral centroid of snoring sounds decreased significantly. Moreover, there was a borderline negative correlation between ΔNC and spectral centroid change during sleep.

Increased pharyngeal tissue is a risk factor for OSA [87]. Our results provided proof of concept that increases in pharyngeal tissue content and edema may decrease spectral centroid of snoring sounds during sleep. Although spectral centroid in low frequency ranges are not same as the formant frequencies, but our results comply with the results of previous studies that have reported that formant frequencies of snoring sounds was smaller in patients with more severe OSA [17, 50]. These results may demonstrate the potential application of the spectral centroid of snoring sounds to predict the risk of OSA due to increased pharyngeal tissue content. Future studies should consider validating these results in clinical populations with OSA such as obese patients, and patients with fluid retaining condition such as renal or heart failure.

This study has some limitations. Since the study was performed during daytime sleep, the results may not be fully applicable to overnight sleep. Future studies should validate these results in overnight sleep studies. Furthermore, participants slept only in supine position to minimize the effects of posture on OSA severity. Future studies should address the effect of posture on snoring sounds features. In this study, we only considered men, as previous studies from our group have shown that men are more susceptible to the adverse effects of rostral fluid shift than women. Future studies should investigate the relationship between snoring sounds features and pharyngeal tissue content in women, children and obese patients.

In conclusion, this study has demonstrated the concept of developing a non-invasive and convenient measure by spectral centroid of snoring sounds to estimate the increases in NFV and pharyngeal tissue edema during sleep. Once established, snore-driven monitoring of NFV and tissue edema could be used to see its effect on the upper airway collapsibility and OSA severity.

Chapter 4

4 Conclusion and Recommendations for Future Works

4.1 Conclusion

This study demonstrated the potential applications of the snoring sounds features for assessing the effects of upper airway anatomy such as narrowing, length and increased NFV. This study showed that snoring intensity could be used to assess the upper airway narrowing. Furthermore, decreases in the resonance frequencies of the snoring sounds could indicate increases in the upper airway length, which is a risk factor of OSA patient. Moreover, this study provided proof of concept that the effects of increasing fluid accumulation in the neck and increased tissue content around the upper airway could change spectral features of snoring sounds.

The first part of the study demonstrated a subject-specific acoustic model for snoring sounds generation. To the best of our knowledge, there is no previously published work which demonstrates a subject-specific model by incorporating the values of the upper airway parameters obtained directly from the subjects. The variations in the upper airway anatomy during sleep are different from individual to individual. Even it varies from night to night in the same person. Therefore, a general model to assess the upper airway anatomy may not provide accurate information for every individual. So, this study proposed a subject-specific model to attain more accuracy in this regard.

As snoring sounds analysis is non-invasive, cost efficient and convenient, this model could help to understand and determine clinical information from the snoring sounds. The modelling results suggested that snoring sounds intensity was strongly correlated with the narrowing of the upper

airway. This result was also supported by the measured sounds intensity obtained from the recording of the snoring sounds. Furthermore, upper airway narrowing is one of the major factors that cause OSA. Thus, these results demonstrate the potential application of snoring sounds intensity to predict severity of upper airway narrowing in patients with OSA.

Furthermore, the first part of the research suggested that longer upper airway could be associated with smaller resonant frequencies of the snoring sounds and vice versa. OSA patients have a longer upper airway length and thicker tongue with narrower upper airway than healthy people even during wakefulness, therefore the resonant frequency of the snoring sounds would be lower in OSA patients than normal patients. We found similar results that the measured spectral frequencies of the recorded snoring sounds were inversely correlated with the sleep apnea severity. Therefore, this result suggested that resonant frequencies of the snoring sounds might be implemented to screen the upper airway length in patients with sleep apnea.

The second part of the study demonstrated the effects of increases in pharyngeal tissue content on the snoring sounds features, assessed by increases in NFV and NC during sleep. One important finding was that the observed decreases in the spectral centroid of the snoring sounds were significantly correlated with the observed increases of the pharyngeal tissue mass. Therefore, these results are convincing for the potential application of spectral centroid of snoring sounds to assess the effects of pharyngeal tissue content on upper airway narrowing.

The main beneficiaries of this study include patients with sleep apnea and sleep physicians. Snoring sounds can be recorded easily and conveniently by a wearable device. Once validated in a large population, physicians can use such wearable device which records the snoring sounds and can screen for the severity of upper airway narrowing. Furthermore, frequency components

of snoring sounds can be used to estimate various risk factors of OSA such as the increased tissue content around the upper airway, or increased collapsibility of the upper airway.

Furthermore, the outcomes of this study may help the physicians to access the efficiency of sleep apnea treatments. The common treatments of OSA include continuous airway positive pressure (CPAP) or mandibular advancement devices. These devices improve sleep apnea by reducing the upper airway narrowing. If the treatments are efficient, we anticipate the snoring sounds intensity to decrease; thus, physicians would be able to determine the patency of the upper airway and efficiency of the OSA treatments more conveniently.

This study can also benefit a wider range of patients with various severities of upper airway narrowing and breathing disorders during sleep. Current diagnosis of breathing disorders during sleep is based on AHI obtained from polysomnography. However, AHI is not sensitive to distinguish the mild and prolonged narrowing of the upper airway. Therefore, the AHI cannot diagnose diseases like upper airway resistance syndrome, a mild form of upper airway narrowing where frequent arousals occur in absence of apneas and hypopneas [98]. Long term consequences of upper airway resistance syndrome include daytime sleepiness and severe cardiovascular comorbidities [98]. This study has shown that monitoring snoring sounds intensity may be used to estimate various levels of narrowing in the upper airway. Thus, implementation of the results of this study may be used to detect patients with mild upper airway narrowing.

To summarize, this thesis provided a proof of concept that snoring sounds analysis can be used to assess variations in the upper airway anatomy during sleep. These results encourage the use of

snoring sounds analysis based convenient and portable technology for monitoring the pharyngeal tissue content and severity of upper airway narrowing during sleep.

4.2 Limitations

This study had some limitations. First, it was performed only on non-obese men. Obesity is one of the major risk factors of sleep apnea [1] and fluid retention diseases [99]. To remove this confounding effect, we excluded obese men (BMI >30) in this study. Though, we expect that due to increased pharyngeal fat and narrower upper airway, the snoring sounds intensity would be higher in obese population than non-obese population. Furthermore, the increased pharyngeal fat surrounding the upper airway could decrease the centroid frequency of the snoring sounds in obese population.

Second, this study was confined to men only due to availability of a small sample size for the study. We chose male subjects because sleep apnea is more frequent in men than in women. Also, the overnight fluid shift has more effect in increasing the severity of OSA in men than women [42]. Based on our findings, we expect that due to shorter upper airway length [100], formant frequencies of snoring sounds would be higher in women than men.

Third, the study was performed in daytime and participants slept for about two to three hours. However, the sleeping time is usually about seven hours on an average in nighttime. Therefore, the site of obstruction and severity of narrowing may show high variance in nighttime sleep than daytime sleep. Thus, the results obtained from our recorded snoring sounds may not be fully applicable for full night sleep.

Forth, the participants were slept in supine position only. We chose this position because we wanted to exclude the postural effects on severity of OSA. Also, while supine, due to the

gravitational force the upper airway is more susceptible to collapse and severity of OSA is increased. However, future studies should be performed to see the postural effects on snoring sounds features.

In the first part of the study, we proposed a modified acoustic model of the upper airway for snoring sounds generation which was single segment from vellum to glottis. However, nasal and oral cavities may have effect on snoring sounds characteristics. Thus, future studies should address the effects of oral and nasal cavities in snoring sounds.

Furthermore, this study was performed on 20 men which was relatively small. Therefore, the results of the study should be validated in larger population. Nevertheless, our results complies with the results of a recent study by Maimon et al. on a large sample size of 1643 patients which shows that snoring sounds intensity is significantly correlated with the severity of sleep apnea [18]. Although, they did not measure the upper airway area in their population, but patients with more severe sleep apnea has more collapsible and narrower upper airway [1]. Therefore, we expect that in larger population, there will be similar correlation between upper airway narrowing and snoring sounds intensity.

4.3 Recommendations for future work

4.3.1 Investigating the dynamics of the upper airway narrowing during hypopnea by snoring sounds intensity

Greater than 50% decrease in breathing airflow for more than 10 sec. with blood oxygen desaturation of greater than 3% is called a hypopnea [72]. It is believed that there would be gradual increase in upper airway narrowing during a hypopnea. According to the findings of this study, if the above statement is true then the snoring sounds intensity should increase within a

hypopnea event. To validate this hypothesis, a sleep study should be conducted with a system that can observe the percentage of the narrowing in the upper airway during sleep along with the simultaneous recordings of the breathing sounds. Then, the pattern of the snoring sounds intensity during hypopnea should be investigated. Once validated, the snoring sounds intensity may predict the dynamics of the upper airway narrowing during hypopnea.

4.3.2 Investigating the dynamics of the upper airway narrowing before an apnea by snoring sounds intensity

Cessation of breathing for more than 10 sec. is called apnea [72]. Therefore, a complete collapse of the upper airway occurs in an obstructive apnea. Hence, there would be no snoring during apnea as there is no breathing. However, upper airway may narrow significantly prior to the complete cessation of breathing. According to the findings of this study, snoring sounds intensity prior to apnea should be higher than the rest of snoring sounds. To validate this hypothesis, a closer inspection of the snoring sounds pattern prior to the apneas should be performed in future studies. The validation of this hypothesis may lead to predict the apneas beforehand.

4.3.3 Investigating the site of upper airway obstruction based on resonant frequencies of snoring sounds

Resonant frequencies may be used as an indicator of site of upper airway obstruction. The vibration in soft palate generates snoring sounds of below 450 Hz, while pharyngeal wall vibration in base of the tongue generates snoring sounds of above 650 Hz [69]. If we assumed that the upper airway length used in our model was a presentation of distance between site of obstruction and recording microphone, then the upper airway length from microphone to soft palate was longer than the length between microphone and tongue base. The results obtained from our model showed that the upper airway length associated with soft palate was associated

with the frequency of 450 Hz, while length associated with tongue based was associated with 800 Hz. In this way, the site of obstruction may be determined from the resonant frequencies. Future studies should verify this hypothesis.

4.3.4 Improving the proposed model for snoring sounds generation by including the nasal and oral cavities

This study proposed a single segment model of the upper airway from vellum (vibratory source of snoring) to glottis, where the microphone recorded snoring sounds. However, in this model the effects of oral and nasal cavity on snoring sounds generation and propagation were not investigated. Therefore, a multi segment model including oral and nasal cavities might give more accurate insight of the upper airway dynamics. Future studies should measure the area of the oral and nasal cavities and develop a subject specific model of the upper airway including these measurements.

4.3.5 Investigating the results on a larger population including the obese men, women and children

This study was performed only on the non-obese healthy men. As this was a preliminary study, we tried to predict the basic anatomical parameters such as narrowing and length of the upper airway by snoring sounds features. However, this study needs to be validated on a larger population including the obese subjects, women and children.

References

[1] J. A. Dempsey, S. C. Veasey, B. J. Morgan, and C. P. O'Donnell, "Pathophysiology of Sleep Apnea," *Physiol. Rev.,* vol. 90, pp. 47-112, 2010.

[2] K. J. Addison-Brown, A. J. Letter, K. Yaggi, L. A. Mcclure, F. W. Unverzagt, V. J. Howard, *et al.*, "Age differences in the association of obstructive sleep apnea risk with cognition and quality of life," *Journal of sleep research,* vol. 23, pp. 69-76, 2014.

[3] I. Djonlagic and A. Malhotra, "Risk of stroke from sleep apnea in men and women," *Expert review of neurotherapeutics,* vol. 10, pp. 1267-1271, 2010.

[4] J. S. Floras, "Sleep apnea and cardiovascular risk," *Journal of cardiology,* vol. 63, pp. 3-8, 2014.

[5] T. Kasai, J. S. Floras, and T. D. Bradley, "Sleep Apnea and Cardiovascular Disease A Bidirectional Relationship," *Circulation,* vol. 126, pp. 1495-1510, 2012.

[6] A. Sanna, "Obstructive sleep apnoea, motor vehicle accidents, and work performance," *Chronic respiratory disease,* vol. 10, pp. 29-33, 2013.

[7] J. Teran-Santos, A. Jimenez-Gomez, and J. Cordero-Guevara, "The association between sleep apnea and the risk of traffic accidents," *New England Journal of Medicine,* vol. 340, pp. 847-851, 1999.

[8] H. Van Dongen and G. Kerkhof, "Sleep loss and accidents—Work hours, life style, and sleep pathology," *Human sleep and cognition, Part II: clinical and applied research,* vol. 2, p. 169, 2011.

[9] H. M. S. D. o. S. Medicine, "The price of fatigue: the surprising economic costs of unmanaged sleep apnea," ed, December 2016.

[10] T. Young, L. Evans, L. Finn, and M. Palta, "Estimation of the clinically diagnosed proportion of sleep apnea syndrome in middle-aged men and women," *Sleep,* vol. 20, pp. 705-706, 1997.

[11] J. A. Verbraecken and W. A. De Backer, "Upper airway mechanics," *Respiration,* vol. 78, pp. 121-33, 2009.

[12] T. Kasai, S. S. Motwani, D. Yumino, J. M. Gabriel, L. T. Montemurro, V. Amirthalingam, *et al.*, "Contrasting effects of lower body positive pressure on upper airways resistance and partial pressure of carbon dioxide in men with heart failure and obstructive or central sleep apnea," *Journal of the American College of Cardiology,* vol. 61, pp. 1157-1166, 2013.

[13] M.-C. Su, K.-L. Chiu, P. Ruttanaumpawan, S. Shiota, D. Yumino, S. Redolfi, *et al.*, "Lower body positive pressure increases upper airway collapsibility in healthy subjects," *Respiratory Physiology & Neurobiology,* vol. 161, pp. 306-312, 2008.

[14] L. Huang, S. J. Quinn, P. D. Ellis, and J. E. Williams, "Biomechanics of snoring," *Endeavour,* vol. 19, pp. 96-100, 1995.

[15] N. Gavriely, T. R. Shee, D. W. Cugell, and J. B. Grotberg, "Flutter in flow-limited collapsible tubes: a mechanism for generation of wheezes," *Journal of Applied Physiology,* vol. 66, pp. 2251-2261, 1989.

[16] A. Azarbarzin and Z. Moussavi, "Snoring sounds variability as a signature of obstructive sleep apnea," *Medical Engineering & Physics,* vol. 35, pp. 479-485, 2013.

[17] J. A. Fiz, J. Abad, R. Jané, M. Riera, M. A. Mañanas, P. Caminal, *et al.*, "Acoustic analysis of snoring sound in patients with simple snoring and obstructive sleep apnoea," *The European Respiratory Journal,* vol. 9, pp. 2365-2370, 1996.

[18] N. Maimon and P. J. Hanly, "Does snoring intensity correlate with the severity of obstructive sleep apnea?," *J. Clin. Sleep Med. ,* vol. 6, pp. 475-478, 2010.

[19] J. R. Perez-Padilla, E. Slawinski, L. M. Difrancesco, R. R. Feige, J. E. Remmers, and W. A. Whitelaw, "Characteristics of the snoring noise in patients with and without occlusive sleep apnea," *The American Review of Respiratory Disease*, vol. 147, pp. 635-644, 1993.

[20] A. K. Ng, K. Y. Wong, C. H. Tan, and T. S. Koh, "Bispectral analysis of snore signals for obstructive sleep apnea detection," *in proc. of 2007 Annual International Conference of the IEEE Engineering in Medicine and Biology Society*, pp. 6196-6199, 2007.

[21] A. K. Ng, T. S. Koh, E. Baey, T. H. Lee, U. R. Abeyratne, and K. Puvanendran, "Could formant frequencies of snore signals be an alternative means for the diagnosis of obstructive sleep apnea?," *Sleep Medicine*, vol. 9, pp. 894-898, 2008.

[22] A. Azarbarzin and Z. Moussavi, "Snoring sounds' statistical characteristics depend on anthropometric parameters," *Journal of Biomedical Science and Engineering*, vol. 5, p. 245, 2012.

[23] A. K. Ng, T. S. Koh, U. R. Abeyratne, and K. Puvanendran, "Investigation of obstructive sleep apnea using nonlinear mode interactions in nonstationary snore signals," *Ann Biomed Eng*, vol. 37, pp. 1796-806, Sep 2009.

[24] J. Xi, X. Si, J. Kim, G. Su, and H. Dong, "Modeling the pharyngeal anatomical effects on breathing resistance and aerodynamically generated sound," *Med Biol Eng Comput*, vol. 52, pp. 567-77, Jul 2014.

[25] C. M. Rembold and P. M. Suratt, "Airway turbulence and changes in upper airway hydraulic diameter can be estimated from the intensity of high frequency inspiratory sounds in sleeping adults," *J Physiol*, vol. 592, pp. 3831-9, Sep 1 2014.

[26] D. Elad, G. Soffer, U. Zaretsky, M. Wolf, and R. J. Shiner, "Time-frequency analysis of breathing signals: in vitro airway model," *Technol Health Care,* vol. 9, pp. 269-80, 2001.

[27] V. P. Harper, H. Pasterkamp, H. Kiyokawa, and G. R. Wodicka, "Modeling and measurement of flow effects on tracheal sounds," *IEEE transactions on bio-medical engineering,* vol. 50, pp. 1-10, 2003.

[28] Z. S. Liu, X. Y. Luo, H. P. Lee, and C. Lu, "Snoring source identification and snoring noise prediction," *J Biomech,* vol. 40, pp. 861-70, 2007.

[29] A. K. Ng, T. S. Koh, E. Baey, and K. Puvanendran, "Role of upper airway dimensions in snore production: acoustical and perceptual findings," *Ann Biomed Eng,* vol. 37, pp. 1807-1817, 2009.

[30] S. Javaheri, "Sleep disorders in systolic heart failure: a prospective study of 100 male patients. The final report," *Int J Cardiol,* vol. 106, pp. 21-8, Jan 4 2006.

[31] D. Yumino, H. Wang, J. S. Floras, G. E. Newton, S. Mak, P. Ruttanaumpawan, *et al.*, "Prevalence and physiological predictors of sleep apnea in patients with heart failure and systolic dysfunction," *J Card Fail,* vol. 15, pp. 279-85, May 2009.

[32] K. Ferrier, A. Campbell, B. Yee, M. Richards, T. O'Meeghan, M. Weatherall, *et al.*, "Sleep-disordered breathing occurs frequently in stable outpatients with congestive heart failure," *Chest,* vol. 128, pp. 2116-22, Oct 2005.

[33] P. J. Hanly and A. Pierratos, "Improvement of sleep apnea in patients with chronic renal failure who undergo nocturnal hemodialysis," *N Engl J Med,* vol. 344, pp. 102-7, Jan 11 2001.

[34] M. A. Kraus and R. J. Hamburger, "Sleep apnea in renal failure," *Adv Perit Dial,* vol. 13, pp. 88-92, 1997.

[35] C. J. de Oliveira Rodrigues, O. Marson, S. Tufic, O. Kohlmann, Jr., S. M. Guimaraes, P. Togeiro, *et al.*, "Relationship among end-stage renal disease, hypertension, and sleep apnea in nondiabetic dialysis patients," *Am J Hypertens,* vol. 18, pp. 152-7, Feb 2005.

[36] B. Jurado-Gamez, A. Martin-Malo, M. A. Alvarez-Lara, L. Munoz, A. Cosano, and P. Aljama, "Sleep disorders are underdiagnosed in patients on maintenance hemodialysis," *Nephron Clin Pract,* vol. 105, pp. c35-42, 2007.

[37] T. Kasai, T. D. Bradley, O. Friedman, and A. G. Logan, "Effect of intensified diuretic therapy on overnight rostral fluid shift and obstructive sleep apnoea in patients with uncontrolled hypertension," *J Hypertens,* 2013.

[38] S. Redolfi, I. Arnulf, M. Pottier, J. Lajou, I. Koskas, T. D. Bradley, *et al.*, "Attenuation of obstructive sleep apnea by compression stockings in subjects with venous insufficiency," *Am J Respir Crit Care Med,* vol. 184, pp. 1062-6, 2011.

[39] L. H. White, O. D. Lyons, A. Yadollahi, C. M. Ryan, and T. D. Bradley, "Effect of Below-the-knee Compression Stockings on Severity of Obstructive Sleep Apnea: A Randomized Trial," *Sleep Med,* vol. 16, pp. 258-64, 2015.

[40] R. M. Elias, C. T. Chan, N. Paul, S. S. Motwani, T. Kasai, J. M. Gabriel, *et al.*, "Relationship of pharyngeal water content and jugular volume with severity of obstructive sleep apnea in renal failure," *Nephrology, Dialysis, Transplantation: Official Publication of the European Dialysis and Transplant Association - European Renal Association,* vol. 28, pp. 937-944, 2013.

[41] R. M. Elias, T. D. Bradley, T. Kasai, S. S. Motwani, and C. T. Chan, "Rostral overnight fluid shift in end-stage renal disease: relationship with obstructive sleep apnea," *Nephrol Dial Transplant,* vol. 27, pp. 1569-73, 2012.

[42] T. Kasai, S. S. Motwani, D. Yumino, S. Mak, G. E. Newton, and T. D. Bradley, "Differing relationship of nocturnal fluid shifts to sleep apnea in men and women with heart failure," *Circ Heart Fail,* vol. 5, pp. 467-74, 2012.

[43] S. Redolfi, D. Yumino, P. Ruttanaumpawan, B. Yau, M. C. Su, J. Lam, *et al.*, "Relationship between overnight rostral fluid shift and Obstructive Sleep Apnea in nonobese men," *Am J Respir Crit Care Med,* vol. 179, pp. 241-6, 2009.

[44] L. H. White, O. D. Lyons, A. Yadollahi, C. M. Ryan, and T. D. Bradley, "Night-to-night Variability in Obstructive Sleep Apnea Severity: Relationship to Overnight Rostral Fluid Shift," *J Clin Sleep Med.,* vol. 11, pp. 149-56, 2015.

[45] D. Yumino, S. Redolfi, P. Ruttanaumpawan, M. C. Su, S. Smith, G. E. Newton, *et al.*, "Nocturnal rostral fluid shift: a unifying concept for the pathogenesis of obstructive and central sleep apnea in men with heart failure," *Circulation,* vol. 121, pp. 1598-605, 2010.

[46] A. Yadollahi, J. M. Gabriel, L. H. White, L. Taranto Montemurro, T. Kasai, and T. D. Bradley, "A Randomized, Double Cross-over Study to Investigate the Influence of Saline Infusion on Sleep Apnea Severity in Men," *Sleep,* vol. 37, pp. 1699-705, 2014.

[47] O. D. Lyons, C. T. Chan, A. Yadollahi, and T. D. Bradley, "Effect of ultrafiltration on sleep apnea and sleep structure in patients with end-stage renal disease," *Am J Respir Crit Care Med,* vol. 191, pp. 1287-94, 2015.

[48] S. K. Ramachandran, "Can intravenous fluids explain increased postoperative sleep disordered breathing and airway outcomes?," *Sleep,* vol. 37, pp. 1587-8, 2014.

[49] T. D. Lam, M. Singh, and F. Chung, "Salt Content in IV Fluids Given Intraoperatively May Influence Postoperative OSA Severity," *Sleep,* vol. 38, p. 989, 2015.

[50] S. Saha, T. D. Bradley, M. Taheri, Z. Moussavi, and A. Yadollahi, "A Subject-Specific Acoustic Model of the Upper Airway for Snoring Sounds Generation," *Sci Rep*, vol. 6, p. 25730, 2016.

[51] D. Pevernagie, R. M. Aarts, and M. De Meyer, "The acoustics of snoring," *Sleep Med. Rev.*, vol. 14, pp. 131-144, 2010.

[52] J. W. Bloom, W. T. Kaltenborn, and S. F. Quan, "Risk factors in a general population for snoring. Importance of cigarette smoking and obesity," *Chest*, vol. 93, pp. 678-83, 1988.

[53] L. H. White and T. D. Bradley, "Role of nocturnal rostral fluid shift in the pathogenesis of obstructive and central sleep apnoea," *J Physiol*, vol. 591, pp. 1179-93, 2013.

[54] W. J. Randerath, B. M. Sanner, and V. K. Somers, *Sleep apnea: current diagnosis and treatment* vol. 35: Karger Medical and Scientific Publishers, 2006.

[55] D. L. Bliwise, J. C. Nekich, and W. C. Dement, "Relative validity of self-reported snoring as a symptom of sleep apnea in a sleep clinic population," *Chest*, vol. 99, pp. 600-8, 1991.

[56] L. H. White and T. D. Bradley, "Role of nocturnal rostral fluid shift in the pathogenesis of obstructive and central sleep apnoea," *The Journal of Physiology*, vol. 591, pp. 1179-1193, 2013.

[57] A. Yadollahi and Z. M. Moussavi, "A robust method for heart sounds localization using lung sounds entropy," *IEEE Trans. Biomed. Eng.*, vol. 53, pp. 497-502, 2006.

[58] H. Pasterkamp, S. S. Kraman, and G. R. Wodicka, "Respiratory sounds. Advances beyond the stethoscope," *Am. J. Respir. Crit. Care Med.*, vol. 156, pp. 974-987, 1997.

[59] P. Boersma and R. KIRCHNER, "Functional Phonology. Formalizing the interactions between articulatory and perceptual drives," *Glot International*, vol. 4, pp. 13-15, 1999.

[60] P. Harper, S. S. Kraman, H. Pasterkamp, and G. R. Wodicka, "An acoustic model of the respiratory tract," *IEEE transactions on bio-medical engineering*, vol. 48, pp. 543-550, 2001.

[61] G. R. Wodicka, K. N. Stevens, H. L. Golub, E. G. Cravalho, and D. C. Shannon, "A model of acoustic transmission in the respiratory system," *IEEE Trans. Biomed. Eng.*, vol. 36, pp. 925-934, 1989.

[62] Y. Finkelstein, L. Wolf, A. Nachmani, U. Lipowezky, M. Rub, S. a. Shemer, *et al.*, "Velopharyngeal anatomy in patients with obstructive sleep apnea versus normal subjects," *Journal of Oral and Maxillofacial Surgery: Official Journal of the American Association of Oral and Maxillofacial Surgeons*, vol. 72, pp. 1350-1372, 2014.

[63] F. Maltais, G. Carrier, Y. Cormier, and F. Sériès, "Cephalometric measurements in snorers, non-snorers, and patients with sleep apnoea," *Thorax*, vol. 46, pp. 419-423, 1991.

[64] K. K. Paliwal, Spectral subband centroid features for speech recognition, in *Proceedings of the IEEE International Conference on Acoustics, Speech and Signal Processing*,pp. 617-620, 1998.

[65] R. Beck, M. Odeh, A. Oliven, and N. Gavriely, "The acoustic properties of snores," *The European Respiratory Journal*, vol. 8, pp. 2120-2128, 1995.

[66] E. Sforza, W. Bacon, T. Weiss, A. Thibault, C. Petiau, and J. Krieger, "Upper airway collapsibility and cephalometric variables in patients with obstructive sleep apnea," *Am. J. Respir. Crit. Care Med.*, vol. 161, pp. 347-352, 2000.

[67] J. A. Fiz, J. Morera, J. Abad, A. Belsunces, M. Haro, J. I. Fiz, *et al.*, "Acoustic analysis of vowel emission in obstructive sleep apnea," *Chest*, vol. 104, pp. 1093-6, 1993.

[68] M. Robb, J. Yates, and E. Morgan, "Vocal tract resonance characteristics of adults with obstructive sleep apnea," *Acta Otolaryngol.,* vol. 117, pp. 760-763, 1997.

[69] S. J. Quinn, L. Huang, P. D. Ellis, and J. E. Williams, "The differentiation of snoring mechanisms using sound analysis," *Clinical Otolaryngology and Allied Sciences,* vol. 21, pp. 119-123, 1996.

[70] H. Xu, W. Huang, L. Yu, and L. Chen, "Sound spectral analysis of snoring sound and site of obstruction in obstructive sleep apnea syndrome," *Acta Otolaryngol.,* vol. 130, pp. 1175-1179, 2010.

[71] S. A. Clark, C. R. Wilson, M. Satoh, D. Pegelow, and J. A. Dempsey, "Assessment of inspiratory flow limitation invasively and noninvasively during sleep," *American Journal of Respiratory and Critical Care Medicine,* vol. 158, pp. 713-722, 1998.

[72] "Sleep-related breathing disorders in adults: recommendations for syndrome definition and measurement techniques in clinical research. The Report of an American Academy of Sleep Medicine Task Force," *Sleep,* vol. 22, pp. 667-689, 1999.

[73] J. J. Fredberg, M. E. Wohl, G. M. Glass, and H. L. Dorkin, "Airway area by acoustic reflections measured at the mouth," *Journal of Applied Physiology: Respiratory, Environmental and Exercise Physiology,* vol. 48, pp. 749-758, 1980.

[74] A. Yadollahi, F. Rudzicz, S. Mahallati, M. Coimbra, and T. D. Bradley, "Acoustic estimation of neck fluid volume," *Annals of Biomedical Engineering,* vol. 42, pp. 2132-2142, 2014.

[75] A. Yadollahi and Z. M. Moussavi, "A robust method for estimating respiratory flow using tracheal sounds entropy," *IEEE Trans Biomed Eng,* vol. 53, pp. 662-8, 2006.

[76] D. FitzGerald and J. Paulus, "Unpitched percussion transcription," in *Signal Processing Methods for Music Transcription*, ed: Springer, pp. 131-162, 2006.

[77] D. Talkin, "A robust algorithm for pitch tracking (RAPT)," in *Speech coding and synthesis*, ed: Elsevier Sciences, pp. 495-518, 1995.

[78] E. Kaniusas, *Linking physiological phenomena and biosignals*, First ed. Berlin: Springer, 2012.

[79] J. R. Deller, J. H. L. Hansen, and J. G. Proakis, *Discrete-time processing of speech signals*. New York: Institute of Electrical and Electronics Engineers Press, 2000.

[80] M. Brookes, "Voicebox: Speech processing toolbox for matlab," ed, 1997.

[81] G. Fant, *Acoustic Theory of Speech Production*. Paris, France: Mouton, 1970.

[82] J. L. Flanagan, *Speech analysis, synthesis and perception* vol. 3: Springer Science & Business Media, 2013.

[83] R. H. Habib, R. B. Chalker, B. Suki, and A. C. Jackson, "Airway geometry and wall mechanical properties estimated from subglottal input impedance in humans," *J. APPL. PHYSIOL.*, vol. 77, pp. 441-451, 1994.

[84] J. Mansfield and G. Wodicka, "Using acoustic reflectometry to determine breathing tube position and patency," *J. Sound Vibration*, vol. 188, pp. 167-188, 1995.

[85] G. R. Wodicka, K. N. Stevens, H. L. Golub, E. G. Cravalho, and D. C. Shannon, "A model of acoustic transmission in the respiratory system," *Biomedical Engineering, IEEE Transactions on*, vol. 36, pp. 925-934, 1989.

[86] R. Pahkala, J. Seppa, A. Ikonen, G. Smirnov, and H. Tuomilehto, "The impact of pharyngeal fat tissue on the pathogenesis of obstructive sleep apnea," *Sleep Breath*, vol. 18, pp. 275-82, 2014.

[87] I. Katz, J. Stradling, A. S. Slutsky, N. Zamel, and V. Hoffstein, "Do patients with obstructive sleep apnea have thick necks?," *Am Rev Respir Dis,* vol. 141, pp. 1228-31, 1990.

[88] T. Kasai, S. S. Motwani, R. M. Elias, J. M. Gabriel, L. Taranto Montemurro, N. Yanagisawa, *et al.*, "Influence of rostral fluid shift on upper airway size and mucosal water content," *Journal of clinical sleep medicine: JCSM: official publication of the American Academy of Sleep Medicine,* vol. 10, pp. 1069-1074, 2014.

[89] L. H. White, S. Motwani, T. Kasai, D. Yumino, V. Amirthalingam, and T. D. Bradley, "Effect of rostral fluid shift on pharyngeal resistance in men with and without obstructive sleep apnea," *Respiratory Physiology & Neurobiology,* vol. 192, pp. 17-22, 2014.

[90] S. Shiota, C. M. Ryan, K. L. Chiu, P. Ruttanaumpawan, J. Haight, M. Arzt, *et al.*, "Alterations in upper airway cross-sectional area in response to lower body positive pressure in healthy subjects," *Thorax,* vol. 62, pp. 868-872, 2007.

[91] S. Redolfi, I. Arnulf, M. Pottier, T. D. Bradley, and T. Similowski, "Effects of venous compression of the legs on overnight rostral fluid shift and obstructive sleep apnea," *Respiratory physiology & neurobiology,* vol. 175, pp. 390-393, 2011.

[92] A. Azarbarzin and Z. Moussavi, "A comparison between recording sites of snoring sounds in relation to upper airway obstruction," in *Conf Proc IEEE Eng Med Biol Soc.;*, pp. 4246-4249, 2012.

[93] A. Yadollahi, E. Giannouli, and Z. Moussavi, "Sleep apnea monitoring and diagnosis based on pulse oximetery and tracheal sound signals," *Medical & biological engineering & computing,* vol. 48, pp. 1087-1097, 2010.

[94] A. Yadollahi, B. Singh, and T. D. Bradley, "Investigating the Dynamics of Supine Fluid Redistribution Within Multiple Body Segments Between Men and Women," *Annals of Biomedical Engineering,* 2015.

[95] P. Boersma and D. Weenink, "Praat, a system for doing phonetics by computer," *Glot International,* vol. 5, pp. 341-345, 2001.

[96] D. Halliday, R. Resnick, and J. Walker, *Fundamentals of physics extended,* Ninth ed.: John Wiley & Sons, 2010.

[97] C. T. Leondes, *Biomechanical Systems: Techniques and Applications, Volume III: Musculoskeletal Models and Techniques* vol. 3: CRC Press, 2000.

[98] N. Arora, G. Meskill, and C. Guilleminault, "The role of flow limitation as an important diagnostic tool and clinical finding in mild sleep-disordered breathing," *Sleep Science,* vol. 8, pp. 134-142, 2015.

[99] S. Kenchaiah, J. C. Evans, D. Levy, P. W. Wilson, E. J. Benjamin, M. G. Larson, *et al.*, "Obesity and the risk of heart failure," *N Engl J Med,* vol. 347, pp. 305-13, 2002.

[100] M. A. Ma, R. Kumar, P. M. Macey, F. L. Yan-Go, and R. M. Harper, "Epiglottis cross-sectional area and oropharyngeal airway length in male and female obstructive sleep apnea patients," *Nat Sci Sleep,* vol. 8, pp. 297-304, 2016.

[101] F. Dalmasso and R. Prota, "Snoring: analysis, measurement, clinical implications and applications," *The European Respiratory Journal,* vol. 9, pp. 146-159, 1996.

[102] A. D. Lorenzo, A. Andreoli, J. Matthie, and P. Withers, "Predicting body cell mass with bioimpedance by using theoretical methods: a technological review," *the American Physiological Society,* pp. 1542-1558, 1997.

[103] U. G. Kyle, I. Bosaeus, A. D. De Lorenzo, P. Deurenberg, M. Elia, J. M. Gomez, *et al.*, "Bioelectrical impedance analysis--part I: review of principles and methods," *Clin Nutr*, vol. 23, pp. 1226-43, Oct 2004.

[104] K. S. Cole, "Electric impedance of suspensions of spheres," *The Journal of general physiology*, vol. 12, pp. 29-36, 1928.

[105] F. Zhu, M. K. Kuhlmann, G. A. Kaysen, S. Sarkar, C. Kaitwatcharachai, R. Khilnani, *et al.*, "Segment-specific resistivity improves body fluid volume estimates from bioimpedance spectroscopy in hemodialysis patients," *J Appl Physiol*, vol. 100, pp. 717-24, Feb 2006.

[106] XITRON, "HYDRA ECF/ICF (Model 4200),Bio-Impedance Spectrum Analyzer, For Measuring Intracellular And Extracellular Fluid Volumes," XITRON Technologies Inc2007.

Appendix A: Feature Extraction of Snoring Sounds

We extracted several temporal and spectral features for all snoring segments (Table A.1).

A.1. Temporal Features:

Since sleep stage may change the upper airway control mechanism and the generation of snoring sounds[1], we investigated the patterns of snoring occurrences for the entire sleep and every sleep stage separately. We calculated two features: snoring percentage, which represent the number of snoring segments in each sleep stage divided by the total number of snoring segments in the entire sleep; and snoring time index (STI), representing the total snoring time in each sleep stage divided by time spent in each sleep stage.

A.2. Spectral Features:

For calculating spectral features, we first estimated power spectral density (PSD) using welch method with 100 ms hamming window and 50% overlap between adjacent windows. We calculated spectral features for the entire frequency band (100-4000 Hz), and seven sub-bands: 100-150 Hz, 150-450 Hz, 450-600 Hz, 600-1200 Hz, 1200-1800 Hz, 1800-2500 Hz, and 2500-4000 Hz [75].

To remove the effects of heart sounds signal analysis was done for frequencies above 100 Hz as the majority of heart sounds components are below 100 Hz [57].

The choice of the frequency sub-bands was determined based on the frequency ranges of different sources of vibrations. Previous studies have shown that the main frequency range of the snoring sounds generated from soft palate vibration is from 150-450 Hz [69]. On the other hand,

snoring sounds induced by narrowing in the base of the tongue and pharyngeal wall vibration are above 600 Hz up to 1200 Hz [69]. Furthermore, for mixed snores, where both the hard palate and tongue are responsible for inducing sounds, the harmonics of the snoring frequencies could be expanded to 2200 and 3500 Hz [101]. Moreover, the power level beyond 4000Hz for snoring sound is less than 0.1% of total power. Thus, we choose 4000Hz to be our cut-off frequency. Considering all these facts, we choose those seven sub-bands.

Table A.1: Features calculated from the snoring segments

Feature Name	**Equation/ Method**
Snoring Percentage, %	Snoring in Sleep stage/ Total number of snoring
Snoring Time Index, %	Total Snoring Time/ Total Sleeping Time
Average Signal Power, P_{avg} , dB*	$P_{avg}\ (f_l \le f \le f_u) = \sum_{(f_l \le f \le f_u)} p(f)\Delta f$
Relative Signal Power (RSP), %*	$\frac{P(f_l \le f \le f_u)}{P(100 \le f \le 4000)}$
Spectral Centroid (SC), Hz*	$\frac{\sum_{(f_l \le f \le f_u)} f p(f)\Delta f}{P_{avg}\ (f_l \le f \le f_u)}$
Formant Frequencies, Hz	Linear Predictive Coding (LPC) analysis

$p(f)$ = estimated amplitude by power spectral density

f_l = Lower band frequency and f_u = Higher band frequency.

* Feature was computed over the entire frequency band: 100 – 4000Hz and seven sub-bands of the power spectrum: 100, 150; 150, 450; 450, 600; 600, 1200; 1200, 1800; 1800, 2500; 2500-4000 Hz.

From the PSD, we calculated three spectral features. The spectral features included the average power of snoring sounds in each frequency band; relative power, which defines as the average power of snoring segments in each sub-band divided by the average power in entire frequency band (100-4000 Hz); and spectral centroid, which determines the frequency with the maximum power in each frequency band.

Appendix B: A Modified Acoustic Upper Airway Model

B.1. Introduction:

Respiratory sounds have been used for the clinical diagnosis of various diseases such as OSA, asthma, and respiratory infections. Consequently, to better understand the underlying anatomical structure of the respiratory system, the acoustic properties of the respiratory sounds has been modeled [27, 60, 61]. Furthermore, comparisons between model predictions and acoustic measurements performed in several conditions could reveal the underlying mechanisms such as severity of narrowing or site of narrowing of the respiratory system. Harper at el. developed a model of the entire respiratory tract to simulate acoustic features in the frequency range of 100 to 3000 Hz [60]. Afterwards, turbulent sound sources were applied to the acoustic model [27]. In those models, the acoustic sources were estimated from airflow measured at the mouth, and then inputted into the model to simulate acoustic features such as intensity and resonance frequencies of the respiratory sounds. Those researches demonstrated that models of the respiratory tract for respiratory sounds generation could be used to understand the effects of anatomical structures of respiratory system on the respiratory sounds features.

Snoring sounds are another type of respiratory sounds that originate from vibrations of the soft palate and pharyngeal walls as well as the turbulence of airflow due to narrowing in the upper airway [14]. Therefore, the acoustic properties of snoring sounds may have the potential to determine the anatomical structures of the upper airway [29]. Therefore, various acoustic models of the respiratory tract were developed to determine the effects of variations in respiratory tract anatomy on the acoustic parameters of respiratory sounds [29, 60]. However, these models were developed based on generalized values for the anatomy of the upper airway [27, 60]. However,

upper airway anatomy varies significantly among individuals. For example patients with severe sleep apnea have a narrower upper airway area and longer upper airway than healthy individuals [63]. Therefore, using generalized values without taking into account these specific risk factors may not produce an optimum understating of the upper airway anatomy. To fill this gap, rather than using generalized area or length, values obtained from each individual should be used.

Therefore, our objective in this study was to modify the acoustic model of the upper airway for snoring sounds generation by making it subject specific. To make the model subject specific, we obtained measurements such as upper airway area, length and pharyngeal wall thickness for each subjects and used those measurements in the model. After that, we simulated the response of the model, including its gain and resonance frequencies. The simulation results were compared with the acoustic properties of the recorded snoring sounds, including intensity and resonance frequencies, respectively.

B.2. Method:

A brief description of the previous upper airway acoustic model:

Previous studies have modeled the upper airway as a collapsible tube considering the acoustic losses, heat conduction and wall vibration losses [27, 60]. The electrical equivalent circuit of the upper airway tube is shown in Figure B.1. The impedance type analogy is used to derive the acoustic impedance of the circuit. The impedance type analogy yields the voltage current relationship of a circuit. The acoustic pressure drop of an element is represented by the voltage drop across the electrical element. Here, the pressure drop is relative to the atmospheric pressure. For an applied acoustic pressure drop, there is volume of air movement happens in response. The

velocity of air flow is represented by the electrical current through the circuit. So, the acoustic impedance can be derived by the pressure divided by the air flow speed [27, 60].

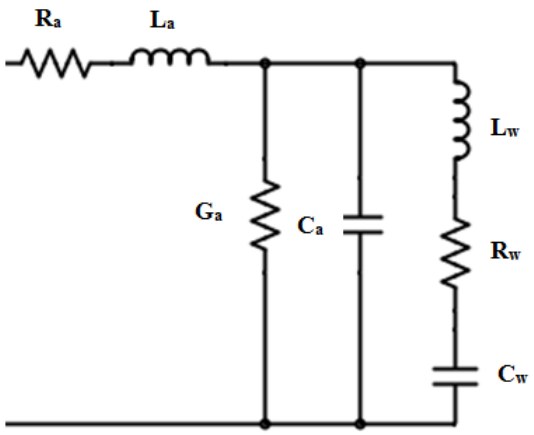

Figure B.1: Electrical equivalent circuit of the upper airway [27, 60]

As the sounds wave propagates along a lossy tube, it experiences the viscous and heat conduction losses and dissipates energy. These losses can be represented by the acoustic resistance (R_a), inertance (L_a), compliance (C_a), and conductance (G_a).

The acoustic resistance (R_a): The acoustic resistance represents a power loss proportional to the velocity square and the power dissipated in viscous friction at the tube wall. Therefore, both the thermal and viscous losses during compressions and expansions of the tube are represented by R_a [81].

The acoustic inertance (L_a): The air mass in the tube has an inertance, which opposes acceleration. The inertance of air mass is analogous to electrical inductance. [81].

The acoustic compliance (C_a): The compliance is analogous to the electrical capacitance. It represents the compressibility of the volume of air contained in a tube. Thus C_a is associated with the ability of air to expand or compress [81].

The acoustic conductance (G_a): The conductance arises from the heat conduction at the walls of the tube [81].

To consider the effects of wall vibration, the wall resistance (R_w), inertance (L_w) and compliance (C_w) are also included in the model [81, 82].

As mentioned previously, the impedance type analogy is used in the circuit, thus the impedance of all the elements in the circuit showed in Figure B.1 is taken into consideration and the final impedance was estimated. Table B.1 shows the equations of all the elements that are derived to model the upper airway.

Table B.1: Equation of the elements of the electrical circuit model of the upper airway (equations and values obtained from [27, 60, 61, 81, 82])

Element	**Formula**
Resistance	$Ra = \frac{2l}{\pi r^3}\sqrt{\frac{\omega I \eta \rho_0}{2}}$
Inertance	$La = \frac{l\rho_0}{A}$
Compliance	$Ca = \frac{Al}{c^2\rho_0}$
Conductance	$Ga = 2\pi rl\frac{v-1}{c^2\rho_0}\sqrt{\frac{k\omega}{2\rho_0 c_p}}$
Wall Resistance	$Rw = \frac{I\eta_w h}{2\pi l r^3}$
Wall Inertance	$Lw = \frac{\rho_w h}{2\pi r l}$
Wall Compliance	$Cw = \frac{2\pi l r^3}{E_w h}$

Density of Median (ρ_0): 1.14e-3 (Moist Air, 37 °C) g/cm^2; Shear Viscosity(Ƞ) : 1.86e-4 (20 Degree, 1 atm) dyne.s/ cm^2; Heat Conduction Coefficient (k): 0.064e-3 (37 °C) cal/cm-S-°C; Ratio of Specific Heat (v = c_p/c$_v$) :1.4; Specific Heat at Constant Pressure(c_p): 0.24 (0 °C, 1 atm)

Cal/g-°C; Speed of Sounds(c): 3.54e4 (Moist Air, 37 °C) cm/s; Tissue Density(ρ_w): 1.06 g/ cm^2; Tissue Viscosity(η_w): 1.6e3 dyne.s/ cm^2; Tissue Elasticity(E_w): 0.392e6 dyne/ cm^2.

Modified subject specific upper airway model for snoring sounds generation:

In this study, we used the previously reported measurements for the air and tissue properties such as viscosity and elasticity (Table B.1).

To make the model subject specific, we used measurements of every individual to modify the input to the model and the elements of the model. We assumed the model input is a sinusoid signal that represents snoring sounds vibration. The frequency of the sinusoid input was considered to be the pitch of the recorded snoring sounds. For every individual, pitch frequency of every snoring segment was estimated and averaged for the entire sleep. To modify elements of the models, for each subject, we measured the upper airway cross sectional area (UA-XSA), distance between velum to glottis before sleep (UA-Length) and neck circumference (NC). From NC and UA-XSA, we estimated the airway wall thickness as follows. From the UA-XSA, we calculated the upper airway radius (T_r) as square root of (UA-XSA/π). We calculated the neck radius (N_r) based on NC as (NC/2π). The wall thickness was calculated as (N_r - T_r).

Thus, in the Table B.1, A = area; $\boldsymbol{r}$ = airway radius; h = wall thickness; l = length; $\boldsymbol{\omega}$ = radian frequency were five parameters which were tuned for each subject to make the model subject specific. Then, we estimated the gain and resonance frequency of the model. Figure B.2 shows the upper airway model with the modification to make it subject specific.

Then, we calculated the effects of changes in UA-XSA, UA-Length and wall thickness on resonance frequencies and gain of the model.

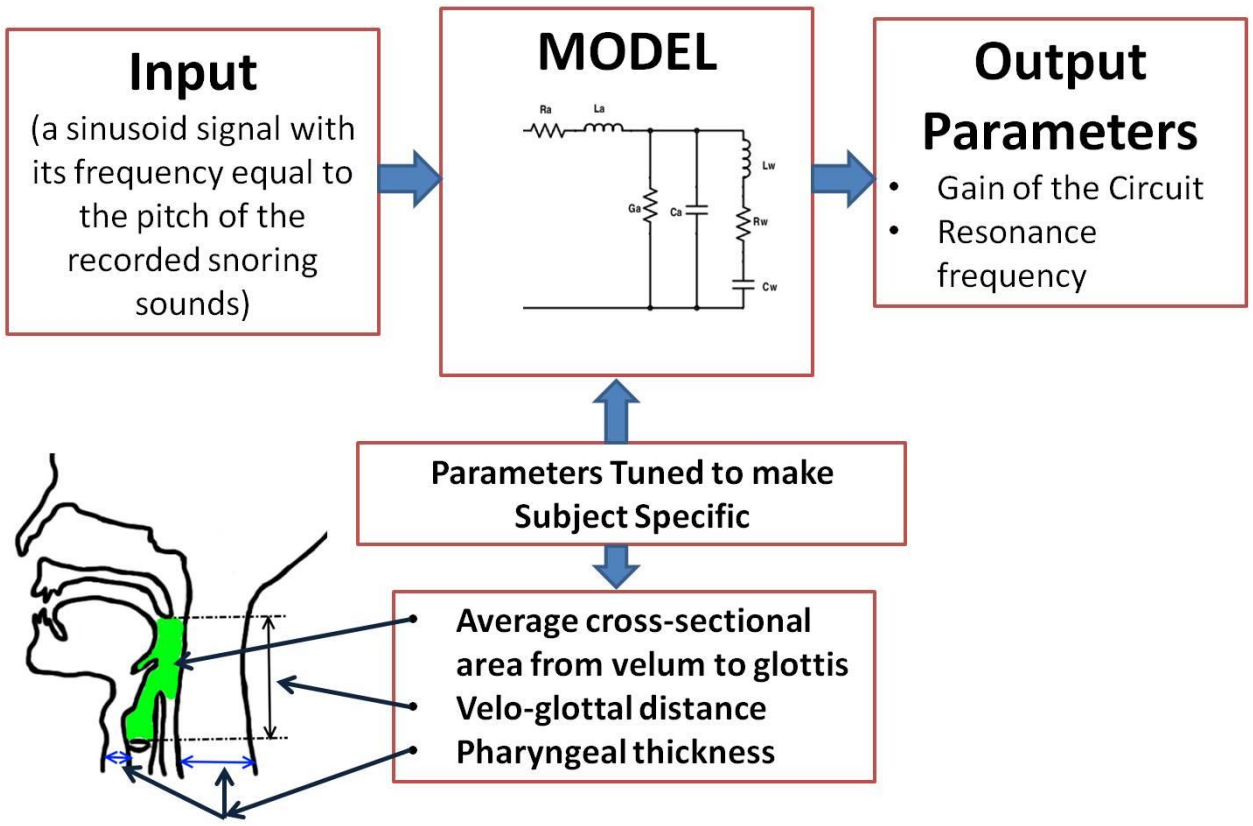

Figure B.2: The modified subject specific upper airway model for snoring sounds generation

B.3. Results:

Table B.2 shows the extracted measurements of the upper airway anatomy before and after sleep, which were used to tune the upper airway model.

Table B.2: Extracted measurements of the upper airway anatomy

Parameter	Symbol	Measured values (mean ± SD)	Range
Cross sectional area	A, cm^2	Before Sleep: 2.62 ± 0.61	Before Sleep: 1.23 to 3.87
		After Sleep: 2.27 ±0.56	After Sleep: 1.02 to 3.24
Radius	r, cm	Before Sleep: 0.9 ± 0.11	Before Sleep: 0.62 to 1.10
		After Sleep: 0.84 ± 0.10	After Sleep: 0.56 to 1.01
Length	l, cm	Before Sleep: 9.06 ± 1.77	Before Sleep: 6 to 12.6
		After Sleep: 9.29 ± 1.75	After Sleep: 6.43 to 12.1
Wall thickness	h, cm	Before Sleep: 5.74 ± 0.46	Before Sleep: 4.9 to 6.8
		After Sleep: 5.90 ± 0.47	After Sleep: 5.1 to 6.8

In the following sections, the effects of UA-XSA, UA-Length and wall thickness on the gain and resonance frequency of the model are described.

Effects of UA-XSA, UA-Length and wall thickness on gain of the model:

In our subjects, the range of changes in UA-XSA measurement in before sleep was 3.87 to 1.23 cm^2 (Table B.2). From the acoustic model, we found the gain of the circuit at resonance frequency was increased from -24.5 dB to -9.6 dB when the UA-XSA decreased from 3.87 to 1.23 cm^2 (Figure B.3 (a)). As demonstrated in Figure B.3 (a), with 2.64 cm^2 narrowing of the upper airway area, there was 14.9 dB increases in gain of the model. However, increases in the thickness of the airway wall (varied from 4.90 to 6.8 cm, Table B. 2) did not affect the gain of the model.

Furthermore, we found that with increases in the UA-Length, there were mild increases in the gain of the circuit (Figure. B.3 (b)).

Effects of UA-XSA, UA-Length and wall thickness on the resonance frequency of the model:

In our subjects, the range of changes in UA-Length measurement in before sleep was 6 to 12.6 cm (Table B.2). From the acoustic model, we found the resonance frequency was decreased from 900 to 450 Hz when the UA-Length of the tube increased from 6 to 12.6 cm (Figure B.4 (a)). Thus, increases in the UA-Length can decrease the resonance frequency and vice versa. Furthermore, Figure B.4 (a) shows that the changes in UA-XSA did not affect the resonance frequency of the circuit.

As illustrated in Figure B.4 (b), variations in the airway wall thickness had no effect on the resonance frequency of the model.

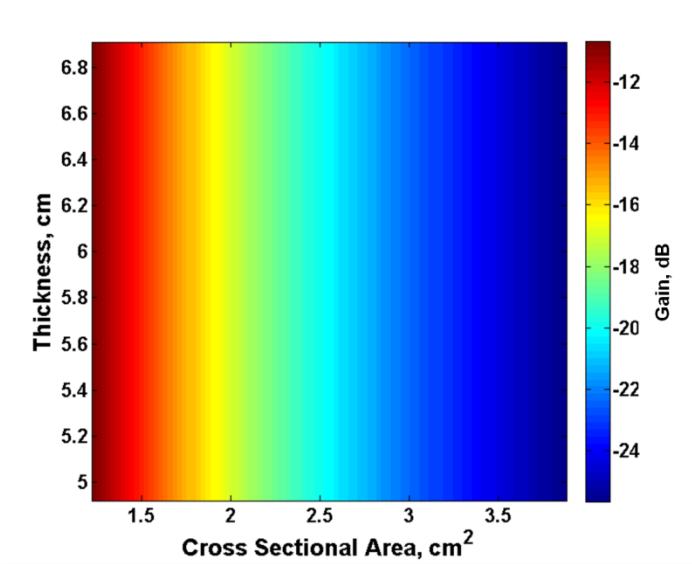

(a)

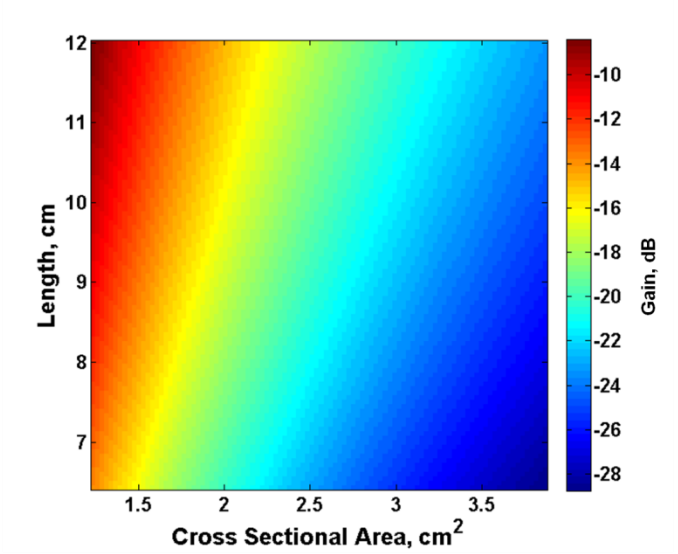

(b)

Figure B.3: (a) Relationship between Gain of the circuit with the cross sectional area and wall thickness; (b) Relationship between Gain of the circuit with the cross sectional area and upper airway length

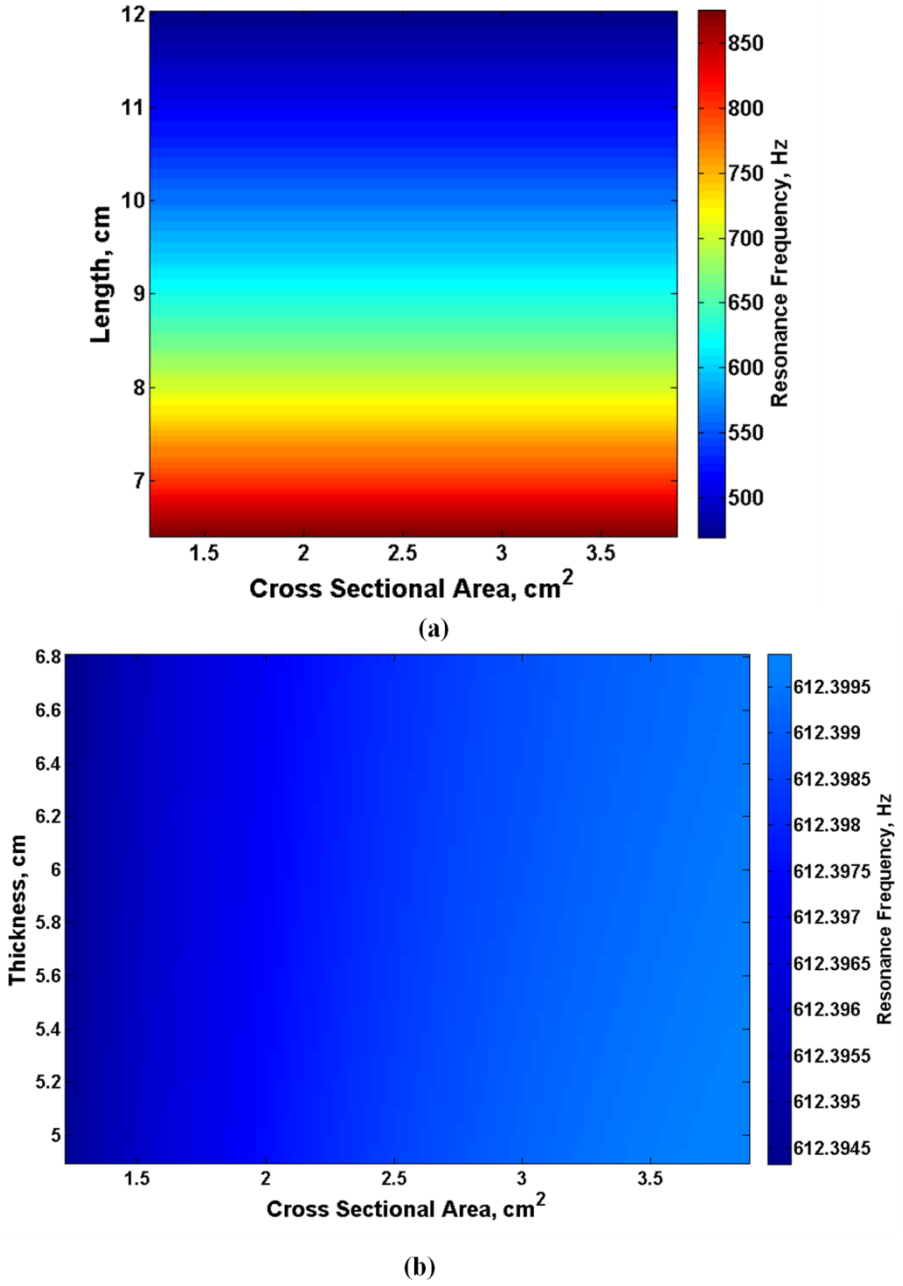

Figure B.4: (a) Relationship between resonance frequency of the model with the cross sectional area and upper airway length; (b) Relationship between resonance frequency of the model with the cross sectional area and wall thickness

B.4. Discussion:

In this study, we proposed a modified subject specific upper airway model for snoring sound generation. We used measurement such as upper airway area, length and wall thickness for each subjects to make the model subject specific. However, we used previously reported values of air or tissue properties in the model. As it was the first approach to make the upper airway model subject specific; we only considered the main anatomical risk factors of sleep apnea such as upper airway area and length. Severe sleep apnea patients usually have a reduced upper airway area and increased upper airway length compared to healthy subjects [62, 63]. Furthermore, anatomical structure such as area and length can change from night to night and even in the same night of sleep. Therefore, the dynamic changes in area or length of the upper airway during sleep should be considered rather than viscous or elastic properties of air or tissue. Thus, by considering these factors, we used upper airway area, length, wall thickness as the main tuning parameters to make the model subject specific.

One of the main outcomes from the model was the inverse relationship between the upper airway area and gain of the model. In this model, we used pitch frequency of the snoring sounds as the input of the circuit. Thus, the gain of the model may be analogous to the simulated intensity of the snoring sounds. Therefore, narrowing in the upper airway can increase the intensity of the snoring sounds.

Another major outcome from the model was that the increases in the length of the upper airway can decrease the resonance frequency of the model. In recorded snoring sounds, formant frequencies were estimated to represent the resonance frequencies. The first formant frequency (F1) of the snoring sounds is associated with the collapsibility of the upper airway between the

vellum and glottis [21]. In our model, we used distance from vellum to glottis as the length of the upper airway. Therefore, our results suggest that increases in the UA-Length can be associated to decreases in the first formant of the snoring sounds.

In conclusion, the proposed subject specific acoustic model of the upper airway for snoring sound generation showed that the area and length of upper airway can change the acoustic characteristics of snoring sounds. This model was the first to show the proof of concept that snoring sound characteristics are associated with the main risk factors of sleep apnea such as narrowing and length of the upper airway. Future studies should validate the results of this model in the clinical population with sleep apnea to estimate the upper airway area and length using snoring sound features.

Appendix C: Bioelectrical Impedance Analysis and Fluid Volume Estimation

C.1. Basics of Bioelectrical Impedance Analysis:

Bioelectrical impedance analysis (BIA) is a technique used to measure various body compositions such as body fat, intra and extracellular fluid volume. In BIA, the impedance is estimated based on Ohm's law by passing a current through the tissue and measuring its voltage. Generally, small amplitude, high frequency sinusoidal current sources are used to form complex impedance (Z). This complex impedance can be presented as the Cartesian form ($Z = R+jX_c$) where R is the resistance (real part) and X_c is the reactance (imaginary part). Also, it can be presented as the Polar form ($Z = |Z|.\exp(j\varphi)$) where |Z| is magnitude and φ is phase angle.

Total impedance of the tissue is affected by the intracellular and extracellular fluid volume. The total impedance (Z) of the tissue segment can be modeled as a resistor in parallel with a series combination of a capacitor and resistor. The capacitor represents the cell membrane (C_m); while the resistors are the intra-cellular fluid (R_{ICW}) and extra-cellular fluid (R_{ECW}) (Figure C.1) [102, 103].

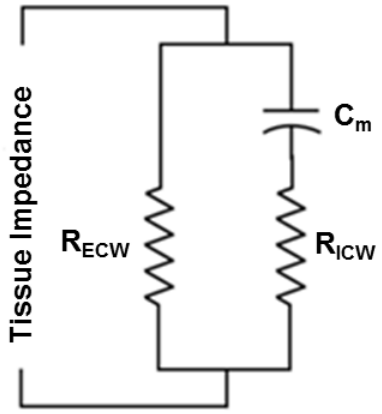

Figure C.1: Electrical model of tissue for BIA; C_m: Cell membrane capacitance, R_{ECW}: Resistance of the extracellular space, R_{ICW}: Resistance of the intracellular space,

At low frequency (<1 kHz), the C_m acts as an insulator and blocks the current passing through the $R_{ICW.}$ Therefore, the measured impedance at low frequency only accounts the resistance of $R_{ECW.}$ At low frequency, the impedance is termed as Z_0. The equation for Z_0 is:

$$Z_0 = R_{ECW} \tag{C1}$$

At very high frequencies (> 1 MHz), C_m acts as a perfect conductor allowing current to pass through both the R_{ICW} and $R_{ECW.}$ So at high frequency, the measured impedance represents the parallel combination of R_{ICW} and R_{ECW}. At very high frequencies, the impedance is termed as $Z_{\infty.}$ The equation for Z_∞ is:

$$Z_\infty = \frac{R_{ICW}R_{ECW}}{[R_{ICW} + R_{ECW}]} \tag{C2}$$

From Eq. C2, the resistance (R) and reactance (Xc) of the model can be expressed as:

$$R = Z_\infty + \frac{[Z_0 - Z_\infty]}{[1 + \omega^2\tau^2]} \tag{C3}$$

$$Xc = -\frac{[\omega\tau(Z_0 - Z_\infty)]}{[1 + \omega^2\tau^2]} \tag{C4}$$

where, $\omega=2\pi f$ and f is the frequency of the current. τ is the time constant and can be expressed as:

$$\tau = C_m[R_{ICW} + R_{ECW}] \tag{C5}$$

Therefore, BIA is highly frequency dependent and changing of frequency changes the measurement of R_{ECW} and R_{ICW}. So to get an accurate measurement, the impedance should be

measured from very low to very high frequencies (e.g. 5kHz-1MHz) [102, 103]. Then, by using the Cole-Cole plot [104] and extrapolation method, the Z_0 and Z_∞ can be estimated. From these estimated values the C_m, R_{ECW} and R_{ICW} can be calculated using equations C1-C5 at a specific frequency. However, in single frequency measurement a small amplitude and high frequency (usually 50 kHz) current is injected into the body to measure the impedance. Previous studies have shown that at 50 kHz, the measurement is a mixture of extracellular and intracellular (~25%) resistances [103]. Therefore, this method is usually used to estimate the extracellular fluid as most of the measurement consists of extracellular fluid.

C.2. Fluid Volume Estimation by BIA:

Estimation of the fluid content of a body segment can be done using BIA by modelling the segment as a cylinder. In the cylinder, the resistance is proportional to its length, and inversely proportional to its diameter as demonstrated in the following equation.

$$R = \frac{\rho L}{A} = \frac{\rho L^2}{V} \tag{C6}$$

where **R** represents the resistance, **L** is the length of the cylinder, **A** is the cross-sectional area, **V** is the volume, and **ρ** is the resistivity [105].

However, the simple cylinder model is not accurate. More accurate models have been achieved by considering each body segment as a truncated cone [106]. The resistance (R) and volume (V_{Total}) of a truncated cone can be expressed as:

$$R = \frac{\rho h}{\pi a b} \tag{C7}$$

$$V_{Total} = \frac{\pi}{3} h[b^2 + a^2 + ab] \tag{C8}$$

where h represents the height of the cone; a, b represent the small and large radius, respectively. V_{Total} represents the total fluid of the segment. In Eq. C7, ρ is the total resistivity of the segment which can be obtained by the following equation:

$$\rho = \frac{\rho_{ECW}}{\left(\frac{V_{ECW}}{V_{Total}}\right)^{3/2}} \tag{C9}$$

where, ρ_{ECW} is the conducting fluid, V_{ECW} is the volume of conducting fluid.

By combining equations C7-C9 the following equation which represents the volume of conducting fluid can be derived [74].

$$V_{ECW} = \frac{(\rho_{ECW})^{2/3}}{3(4\pi)^{1/3}} \left(\frac{h}{R(Cir1)(Cir2)}\right)^{2/3} h((Cir1)^2 + (Cir2)^2 + (Cir1)(Cir2)) \tag{C10}$$

Where Cir1 and Cir2 represent the small and large circumferences of the cone, respectively and ρ_{ECW} represents the resistivity of the extracellular fluid, which has been estimated to be 47 Ohm-cm[102]. Eq. C10 can be further simplified if the circumference of the top and bottom of the segment are considered equal [74].

$$V_{ECW} = \left(\frac{{\rho_{ECW}}^2 h^5 (CIR)^2}{4\pi R^2}\right)^{1/3} \tag{C11}$$

Where CIR = Cir1 = Cir2. In this study, Eq. C11 was used to measure the neck fluid volume from before to after sleep.

Appendix D: Study Protocol and Data Measurement

This study was part of a randomized, double cross-over protocol to investigate the effects of fluid overloading by saline infusion on sleep apnea severity in men [46]. In this study, we used data from the control arm of the original study. The study protocol of original study and data measurement are briefly described below.

D.1. Sleep Study and Polysomnography (PSG):

Daytime PSG was performed for the convenience of participants and the research personnel. Participants were voluntarily sleep deprived to less than 4 hours the night before the study day to induce sleepiness in daytime. Scoring sleep stages and arousals were done by specialist using standard techniques and criteria. Thoracoabdominal motion, nasal pressure, and arterial oxyhemoglobin saturation (SaO_2) were monitored by respiratory inductance plethysmography, nasal cannulae, and oximetry, respectively [71]. The definition and classification of apneas (cessation of airflow to the lungs for at least 10s) and hypopneas (>50% decrease in breathing airflow for more than 10s with blood oxygen desaturation of >3%) were done in accordance with previous standard [72]. The AHI was calculated as the number of apneas and hypopneas per hour of sleep. The participants slept in the supine position with a single foam pillow to eliminate any effects of postural changes on AHI and sleep structure.

D.2. Upper Airway Cross Sectional Area (UA-XSA) Measurement:

UA-XSA was measured using the acoustic pharyngometry [73]. UA-XSA was measured before the subjects fall sleep and as soon as the subjects woke up from the sleep. In both cases, the measurements were done in supine position with no pillow (Figure D.1-a); we made sure the

head was in a neutral position. The measurements were repeated 4 times and reported UA-XSA was the average of these 4 measurements.

D.3. Neck Circumference (NC) Measurement:

NC was assessed just above the circothyroid cartilage by a measuring tape. Similar to UA-XSA, NC was also measured before and after sleep with no pillow. A line was drawn just above the cricothyroid cartilage to maintain the measurements at the same level in both before and after sleep (Figure D.1-b).

D.4. Neck Fluid Volume (NFV) Measurement:

During the study protocol, bioelectrical impedance parameters of the neck were measured using the MP150 and EBI100C modules (Biopac Inc, Goleta, CA) before and after the sleep while the subjects were supine. Two electrodes, which were used to measure voltage, were placed on the right side of the neck below the right ear and at the base of the neck. Two more electrodes were placed 2.5cm apart from the voltage measuring electrodes to inject a 400μA sinusoidal current at a 50 kHz frequency (Figure D.1-c). NFV was estimated using Eq. C11 described in Appendix C; where CIR was the measurement of NC, h was the neck length, R was the resistance that was estimated from the bioelectrical impedance measurements and resistivity (ρ) was 47Ωcm. Since our estimated fluid was mainly affected by the extra-cellular fluid; resistivity of the extra-cellular fluid was used [102]. With subjects in the standing position and having their head in the neutral position, neck length (h) was measured as the distance between the voltage sensing electrodes (Figure D.1-c).

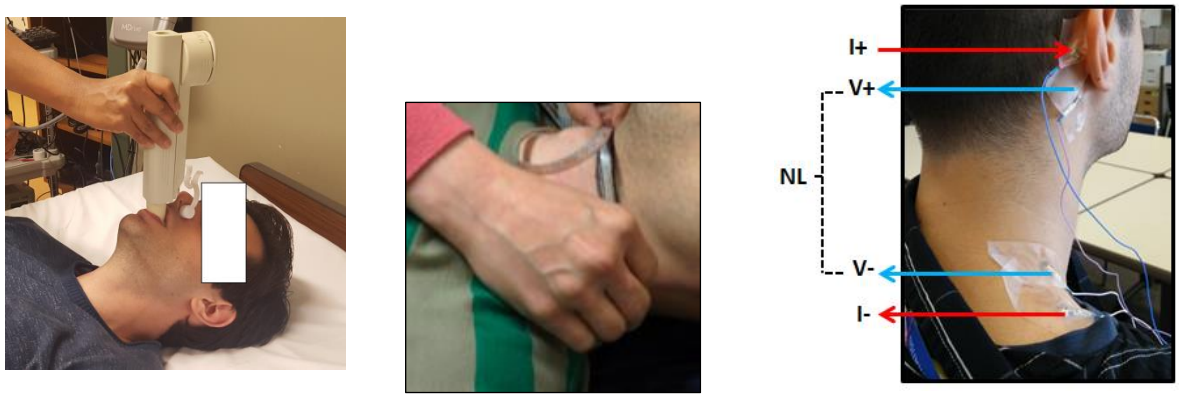

(a) **(b)** **(c)**

Figure D.1: a) UA-XSA Measurement; b) NC Measurement; c) Electrode placement for measuring bioelectrical impedance of the neck (NL: Neck length).

D.5. Breathing Sound Measurement:

Breathing and snoring sounds were recorded by a Sony EMC-44B omni-directional microphone. The microphone was placed over suprasternal notch using double-sided adhesive tape. Biopac DA100C was used for filtering the sounds and a low pass filter was used whose cut-off frequency was 5 kHz. The filtered sounds were then digitized by Biopac MP150 at a sampling frequency of 12.5 kHz.

D.5. Study Protocol:

Participants arrived in the sleep laboratory at late noon after a night of sleep deprivation and were instrumented for sleep studies. In the original study, a negligible amount (approximately 100 ml) of saline was infused by an intravenous cannula during the sleep to keep the vein open in the control arm of the protocol. On the contrary, in the intervention arm approximately 2,000 ml of saline was infused as a bolus just after sleep onset. The saline solution was warmed to body temperature by placing the bag containing the solution in warm water at 37° C. Randomization of participants into a control or intervention arm was done by a computer-generated randomization table with unequal blocks of 2 and 4. Personnel analyzing the results were kept blind to randomization. Baseline measurements including UA-XSA, NC, and NFV were done in supine position before sleep and just after the participants woke up. Respiratory and snoring sounds were recorded continuously during sleep. Participants were crossed over to the other arm of the study one week after the initial session. The Research Ethics Board of Toronto Rehabilitation Institute approved the protocol and all subjects signed consent from prior to participation [46].